COMPARISON OF BUILD-UP REGION DOSES IN OBLIQUE TANGENTIAL 6 MV PHOTON BEAMS CALCULATED BY AAA AND CCC ALGORITHMS IN BREAST RANDO PHANTOM

PONGAPISIT MASUNUN

**A THESIS SUBMITTED IN PARTIAL FULFILLMENT
OF THE REQUIREMENTS FOR
THE DEGREE OF MASTER OF SCIENCE
(MEDICAL PHYSICS)
FACULTY OF GRADUATE STUDIES
MAHIDOL UNIVERSITY
2016**

Thesis
entitled

COMPARISON OF BUILD-UP REGION DOSES IN OBLIQUE TANGENTIAL 6 MV PHOTON BEAMS CALCULATED BY AAA AND CCC ALGORITHMS IN BREAST RANDO PHANTOM

Pongapisit Masunun
.....
Mr. Pongapisit Masunun
Candidate

Puangpen Tangboonduangjit
.....
Lect. Puangpen Tangboonduangjit,
Ph.D. (Medical Radiation Physics)
Major advisor

Nuanpen Damrongkijudom
.....
Lect. Nuanpen Damrongkijudom,
Ph.D. (Medical Radiation Physics)
Co-advisor

.....
Prof. Patcharee Lertrit,
M.D., Ph.D. (Biochemistry)
Dean
Faculty of Graduate Studies
Mahidol University

Puangpen Tangboonduangjit
.....
Lect. Puangpen Tangboonduangjit,
Ph.D. (Medical Radiation Physics)
Program Director
Master of Science Program in
Medical Physics
Faculty of Medicine
Ramathibodi Hospital
Mahidol University

Thesis
entitled

COMPARISON OF BUILD-UP REGION DOSES IN OBLIQUE TANGENTIAL 6 MV PHOTON BEAMS CALCULATED BY AAA AND CCC ALGORITHMS IN BREAST RANDO PHANTOM

was submitted to the Faculty of Graduate Studies, Mahidol University
for the degree of Master of Science (Medical Physics)
on
July 14, 2016

Pongapisit Masunun
.....
Mr. Pongapisit Masunun
Candidate

Taweap Sanghangthum
.....
Lect. Taweap Sanghangthum,
Ph.D. (Nuclear Engineering)
Chair

Puangpen Tangboonduangjit
.....
Lect. Puangpen Tangboonduangjit,
Ph.D. (Medical Radiation Physics)
Member

Nuanpen Dr
.....
Lect. Nuanpen Damrongkijudom,
Ph.D. (Medical Radiation Physics)
Member

.....
Prof. Patcharee Lertrit,
M.D., Ph.D. (Biochemistry)
Dean
Faculty of Graduate Studies
Mahidol University

.....
Prof. Piyamitr Sritara,
M.D., FRCPT, FACP, FRCP
Dean
Faculty of Medicine
Ramathibodi Hospital
Mahidol University

ACKNOWLEDGEMENTS

I would like to express my deepest gratitude to my major advisor, Lect. Puangpen Tangboonduangjit for her very valuable advice, guidance, supervision, constructive comments and patience throughout this thesis. I am grateful to Lect. Nuanpen Damrongkijudom for her important suggestions and comments.

I would also like to thank Medical physicists, Ms. Siwaporn Sakulsingharoj and Ms. Supaporn Srisuwan for their great assistance and training of the techniques through the TLD calibration and TLD reading process. I would also like to show my appreciation to Ms. Pimolpun Changkaew for her training of the use computerized treatment planning system both Eclipse and Pinnacle, and the assistance in ClinaciX using through the irradiation process.

I am grateful to the department of Therapeutic Radiology, Ramathibodi Hospital for allowing in equipment for this experiment. I wish to thank all teachers, lecturers, my classmates and staffs in the School of Medical Physics, Ramathibodi Hospital, Mahidol University for their kind support throughout the entire course of study.

Finally, I am deeply grateful to my family for their financial support, entirely care, and love. The usefulness of this thesis, I dedicate to my family and all teachers who have taught me since my childhood.

Pongapisit Masunun

COMPARISON OF BUILD-UP REGION DOSES IN OBLIQUE TANGENTIAL 6 MV PHOTON BEAMS CALCULATED BY AAA AND CCC ALGORITHMS IN BREAST RANDO PHANTOM

PONGAPISIT MASUNUN 5436421 RAMP/M

M.SC. (MEDICAL PHYSICS)

THESIS ADVISORY COMMITTEE: PUANGPEN TANGBOONDUANGJIT, Ph.D., NUANPEN DAMRONGKIJUDOM, Ph.D.

ABSTRACT

The purpose of this study was to compare the build-up region doses on breast Rando phantom surface with the bolus covered, the doses in breast Rando phantom and also the doses in lung that is the heterogeneous region by two algorithms.

The analytical anisotropic algorithm (AAA) version 8.9 in Eclipse treatment planning system and the collapsed cone convolution (CCC) algorithm version 9.2 in Pinnacle treatment planning system were used to plan in tangential field technique with 6 MV photon beam at 200 cGy total doses in breast Rando phantom with bolus covered (5 mm and 10 mm). Thermoluminescent dosimeters (TLDs) were calibrated with Cobalt-60 and used to measure the doses in irradiation process.

The results in treatment planning showed that the doses in build-up region, the doses in breast phantom and the doses in lung (point L1) were closely matched in both algorithms and both thicknesses of bolus which were less than 2% different. The planning doses in build-up region, breast Rando phantom and lung (point L1) were overestimated in both thicknesses of bolus and both algorithm when compared with irradiated dose except in the lung (point L2) that was a point of beam edges region.

Above all, the TLD measurements showed that CCC algorithm performed better when compared with AAA algorithm at both thicknesses of bolus. However, uncertainties in measurement may occur through the process of placing bolus over the curve of breast Rando phantom which creates an air gap between bolus and surface of the phantom. Further study might be required in other detectors or other techniques to have more evidence to illustrate the accuracy of dose calculation in buildup region and in lung tissue from the algorithms.

KEY WORDS: BUILD-UP REGION / AAA ALGORITHM / CCC ALGORITHM / THERMOLUMINESCENT DOSIMETER / RANDO PHANTOM

46 pages

การเปรียบเทียบปริมาณรังสีบริเวณบิลด์อัพในการฉายรังสีโฟตอน 6 เมกะโวลต์แบบมุมเฉียงระหว่างการคำนวณด้วยอัลกอริทึ่ม AAA กับ CCC ในแรนโดแฟนทอมบริเวณเต้านม

COMPARISON OF BUILD-UP REGION DOSES IN OBLIQUE TANGENTIAL 6 MV PHOTON BEAMS CALCULATED BY AAA AND CCC ALGORITHMS IN BREAST RANDO PHANTOM

พงษ์อภิสิทธิ์ มะสุนัน 5436421 RAMP/M

วท.ม. (ฟิสิกส์การแพทย์)

อาจารย์ที่ปรึกษาวิทยานิพนธ์: พวงเพ็ญ ตั้งบุญดวงจิตร, Ph.D., นวลเพ็ญ ดำรงกิจอุดม, Ph.D.

บทคัดย่อ

การศึกษานี้มีวัตถุประสงค์เพื่อต้องการเปรียบเทียบปริมาณรังสีบริเวณบิลด์อัพบนแรนโดแฟนทอมส่วนเต้านมที่มีโบลัสคลุมอยู่ ปริมาณรังสีในแรนโดแฟนทอมส่วนเต้านมและปริมาณรังสีในบริเวณปอด โดยเปรียบเทียบการคำนวณปริมาณรังสีด้วยอัลกอริทึ่มสองชนิด ได้แก่ อัลกอริทึ่ม AAA ในระบบวางแผนการรักษาของ Eclipse เวอร์ชั่น 8.9 และอัลกอริทึ่ม CCC ในระบบวางแผนการรักษาของ Pinnacle เวอร์ชั่น 8.9 ซึ่งทำการวางแผนการฉายรังสีโฟตอนพลังงาน 6 เมกะโวลต์ ด้วยเทคนิคแบบมุมเฉียง และให้ปริมาณรังสี 200 เซ็นติเกรย์ ในแรนโดแฟนทอมที่มีโบลัสคลุมอยู่ 5 และ 10 มิลลิเมตร อีกทั้งยังมีการวัดปริมาณรังสีที่ได้รับจริงโดยใช้ทีแอลดี (TLD) ซึ่งเป็นตัววัดรังสีชนิดหนึ่งที่มีการสอบเทียบความถูกต้องในการนับวัดรังสีด้วยเครื่องโคบอลต์-60

ผลการศึกษาพบว่า ทั้งสองอัลกอริทึ่มสามารถคำนวณปริมาณรังสีบริเวณบิลด์อัพบนแรนโดแฟนทอมส่วนเต้านมที่มีโบลัสคลุมอยู่ ปริมาณรังสีในแรนโดแฟนทอมส่วนเต้านมและปริมาณรังสีในบริเวณปอด (จุด L1) ได้ใกล้เคียงกันที่โบลัส 5 และ 10 มิลลิเมตร โดยมีค่าความแตกต่างกันน้อยกว่า 2% ยกเว้นบริเวณปอด (จุด L2) ซึ่งมีค่าความแตกต่างมากกว่า 2% และจากการวัดปริมาณรังสีจริงด้วยทีแอลดีพบว่า ปริมาณรังสีบริเวณบิลด์อัพบนแรนโดแฟนทอมส่วนเต้านมที่มีโบลัสคลุมอยู่ ปริมาณรังสีในแรนโดแฟนทอมส่วนเต้านมและปริมาณรังสีบริเวณปอด (จุด L1) ได้ค่าปริมาณรังสีที่น้อยกว่าเมื่อเปรียบเทียบกับปริมาณรังสีที่ได้การคำนวณด้วยอัลกอริทึ่มทั้งสองชนิดในระบบวางแผนการรักษา ยกเว้นบริเวณปอด (จุด L2) ซึ่งมีคลาดเคลื่อนสูงในการวัดปริมาณรังสี เนื่องจากเป็นบริเวณของขอบลำรังสี

จากการศึกษาโดยรวมแล้วพบว่า อัลกอริทึ่ม CCC สามารถที่จะคำนวณปริมาณรังสีในแผนการรักษาได้ใกล้เคียงกับการวัดจริงด้วยตัววัดทีแอลดีมากกกว่าอัลกอริทึ่ม AAA แต่อย่างไรก็ตาม การศึกษาในครั้งนี้ยังมีข้อผิดพลาดบางประการที่อาจทำให้เกิดความคลาดเคลื่อนในการวัดปริมาณรังสี โดยการวางแผ่นโบลัสลงบนแรนโดแฟนทอมส่วนเต้านมนั้น ไม่สามารถทำให้แผ่นโบลัสแนบสนิทชิดกับแรนโดแฟนทอม จึงทำให้เกิดช่องว่างและมีอากาศอยู่ในบริเวณนั้น ทำให้ปริมาณรังสีในบริเวณดังกล่าวคลาดเคลื่อนไป และหากมีการศึกษาครั้งต่อไป ควรจะมีการนำเครื่องวัดปริมาณรังสีชนิดอื่นหรือเทคนิคอื่นๆเข้ามาประยุกต์ใช้ เพื่อความถูกต้องแม่นยำในการวัดและคำนวณปริมาณรังสีบริเวณดังกล่าว

46 หน้า

CONTENTS

		Page
ACKNOWLEDGEMENTS		**iii**
ABSTRACT (ENGLISH)		**iv**
ABSTRACT (THAI)		**v**
LIST OF TABLES		**vii**
LIST OF FIGURES		**ix**
LIST OF ABBREVIATIONS		**x**
CHAPTER I	**INTRODUCTION**	**1**
CHAPTER II	**OBJECTIVES**	**3**
CHAPTER III	**LITERATURE REVIEWS**	**4**
CHAPTER IV	**MATERIALS AND METHODS**	**9**
CHAPTER V	**RESULTS AND DISCUSSION**	**16**
CHAPTER VI	**CONCLUSIONS**	**24**
REFERENCES		**25**
APPENDIX		**27**
BIOGRAPHY		**46**

LIST OF TABLES

Table		Page
3.1	Field border of tangential field technique	5
4.1	A parameter of technique planning in both thicknesses of bolus and both algorithms	13
5.1	Irradiated doses and the average of absolute doses from TLD group 1 reading	16
5.2	Irradiated doses and the average of absolute doses from TLD group 2 reading	17
5.3	Irradiated doses and the average of absolute doses from TLD group 3 reading	17
5.4	A comparison of point doses in treatment planning by AAA algorithm (Eclipse) versus CCC algorithm (Pinnacle) in breast Rando phantom with 5 mm and 10 mm bolus covered	19
5.5	A comparison of point doses from treatment planning doses versus TLD measurements in breast Rando phantom with 5 mm bolus thicknesses covered in both algorithms	21
5.6	A comparison of point doses from treatment planning doses versus TLD measurements in breast Rando phantom with 10 mm bolus thicknesses covered in both algorithms	22
A.1	The ECC_i value of each TLD in group 1	28
A.2	The ECC_i value of each TLD in group 2	30
A.3	The ECC_i value of each TLD in group 3	32
A.4	The ECC_{ci} value of each TLD in group 1	35
A.5	The ECC_{ci} value of each TLD in group 2	38
A.6	The ECC_{ci} value of each TLD in group 3	39

LIST OF TABLES (cont.)

Table		Page
A.7	The point doses in treatment planning by both algorithms calculation with 5 mm bolus covered	43
A.8	The point doses in treatment planning by both algorithms calculation with 10 mm bolus covered	44
A.9	The irradiated doses in breast Rando phantom with 5 mm bolus covered by both algorithms calculation	44
A.10	The irradiated doses in breast Rando phantom with 10 mm bolus covered by both algorithms calculation	45

LIST OF FIGURES

Figure		Page
4.1	The Varian ClinaciX linear accelerator	9
4.2	The GE Optima CT580 Healthcare in Ramathibodi Hospital	10
4.3	The Alderson Rando phantom	11
4.4	The TLD annealing oven and TLD Reader	11
4.5	The 5 and 10 mm thicknesses of bolus	12
4.6	The points of TLD in breast Rando phantom slab, the points of TLD in lung and on the surface with bolus covered	14
4.7	The Varian ClinaciX in irradiation process	15
5.1	The linearity test for TLD group 1	16
5.2	The linearity test for TLD group 2	17
5.3	The linearity test for TLD group 3	18
5.4	The percentage difference of point doses in treatment planning between AAA and CCC at both bolus thicknesses	19
5.5	The graph of percentage difference between planning doses versus irradiated doses in both algorithms at 5 mm bolus thicknesses	21
5.6	The graph of percentage difference between planning doses versus irradiated doses in both algorithms at 10 mm bolus thicknesses	22
5.7	The lung point L2 which located through the beam edges	23
A.1	The dose distribution in breast Rando phantom with 5 and 10 mm bolus covered by AAA algorithm (Eclipse TPS)	42
A.2	The dose distribution in breast Rando phantom with 5 and 10 mm bolus covered by CCC algorithm (Pinnacle TPS)	43

LIST OF ABBREVIATIONS

Abbreviation	Term
AAA	Analytical anisotropic algorithm
CCC	Collapsed cone convolution
cGy	Centigray
cm	Centimeter
cm^2	Square centimeter
CT	Computed tomography
D_{max}	Depth of dose maximum
D_u	Unknown dose
ECC_{ci}	Individual element correction coefficient
ECC_i	Element Correction Coefficient
FPG	Full phantom geometry
Gy	Gray
HPG	Half phantom geometry
MeV	Mega electron volt
MLC	Multi-leaf collimator
mm	Millimeter
MU	Monitor unit
MV	Megavoltage
nC	Nanocoulomb
pGy	Picogray
PSD	Percent surface dose
PTV	Planning target volume
Q_{ci}	Correct charge integral
Q_i	Individual charge reading of each TLD
RCF	Reader calibration factor

LIST OF ABBREVIATIONS (cont.)

Abbreviation	Term
SAD	Source to axis distance
SD	Standard deviation
TERMA	Total energy released per unit mass
TLD	Thermoluminescent dosimeter
TPS	Treatment planning system
% Diff	Percentage difference
˚C	Celsius degree

CHAPTER I
INTRODUCTION

Radiation is currently important in the medical field that used for diagnostic and treating the patients, especially in cancer patients. The delivered radiation doses to the patients must be precise, accurate and appropriate for the local of any type of cancer. The evaluation of delivered doses on surface area, in build-up region or in the heterogeneous medium is quite uncertain due to the algorithm calculation that may cause the effect directly to the patients such as erythema and hyperpigmentation. Too low doses from the uncertain calculation are insufficient to damage the gross tumor or too high doses are over limited for curing cancer and affected to the result of treatment.

Nowadays, new technologies of treatment machines are developed due to the complex of planning and treatment. Dose calculation algorithms are influential and controlled the accuracy of radiation doses in treatment planning process. In all superposition/convolution methods, the analytical anisotropic algorithm (AAA) and the collapsed cone convolution algorithm (CCC) are popular because of the accuracy in heterogeneous media calculation, especially in the lung. However, both algorithms can not well predict the surface doses and build-up region doses in solid water phantom shown by the study of Chow et al [1]. On the other hand, the study by Hasenbalg et al [2] have shown that CCC algorithm performed overall better than AAA algorithm compared to Monte Carlo in clinical cases of lung and breast.

Mostly irradiation treatment in breast cancer case is oblique tangential photon beam technique. The prediction of surface doses variation for the tangential like photon beams are extremely caution in radiation therapy. Chow and Grigorov [3] have shown that the relative dose profile in the phantom skin did not change with oblique beam using full phantom geometry. Nevertheless, the surface relative depth dose was increased for half phantom geometry (phantom-air interface) like the breast. Above all, in this study is to compare the build-up region doses on breast Rando phantom surface with the bolus covered, the doses in breast Rando phantom and also

the doses in lung by two algorithms which are analytical anisotropic algorithm and collapsed cone convolution algorithm.

Above all, the treatment planning was used and predicted the radiation doses from both algorithms calculation. However, the actual radiation doses should be measured directly by the suitable dosimeter for comparing the difference of estimated doses and measured doses. The suitable dosimeter was thermoluminescent dosimeters (TLDs) that calibrated with Cobalt-60 and used to measure the doses in irradiation process.

CHAPTER II
OBJECTIVE

The main objectives of this study are to compare the build-up region doses on breast Rando phantom surface with the bolus covered, the doses in breast Rando phantom and also the doses in lung by AAA and CCC algorithms. The sub-objective is to study that which algorithm is calculated closer to the direct measurement by thermoluminescent dosimeter (TLD).

CHAPTER III
LITERATURE REVIEWS

3.1 Basic knowledge

3.1.1 Build-up region

The build-up region is a region between the surface and the depth of maximum dose where the high dose gradient rapidly increased. The result of build-up region dose is called “skin sparing effect”. The build-up region is comprised of the primary photon beam, backscattered radiation from the patient and contamination electron.

3.1.2 Thermoluminescent dosimeter

Thermoluminescent dosimetry (TLD) is based on the ability of certain imperfect crystals to absorb and store the energy of ionizing radiation, upon heating, is re-emitted in the form of light. The light is detected and the light output is correlated to the absorbed dose. TLD are generated naturally or by doping phosphors with a very small percentage of activators (LiF:Mg-Ti is lithium fluoride doped with magnesium and titanium, $Li_2B_4O_7$:Cu is lithium borate doped with copper, etc.). They are available in the form of power, solid dosimeters made of polycrystalline extrusions (rods, sintered pellets or chips) or powder bonded to a polypropylene and plastic substrate. TLD can be used for in-vivo dose measurement in external radiotherapy and brachytherapy.

3.1.3 Tangential field technique in breast radiothery

The breast or chest wall is treated isocentrically and covered by a pair of opposing tangential fields. The posterior beam edges are parallel to reduce divergence into the lung. The whole breast is included to ensure any residual or microscopic disease is irradiated. Field border is shown in Table 3.1.

Table 3.1 Field border of tangential field technique.

Field border	Anatomical landmark
Superior border	Suprasternal notch
Inferior border	2 cm lower from the scar
Medial border	Anatomical midline
Lateral border	Midaxiallary line

3.1.4 Analytical Anisotropic Algorithm (AAA)

The AAA is a 3D pencil beam convolution/superposition algorithm and implemented in the Eclipse treatment planning system. Monte Carlo is used to characterize the clinical beam and to model the basic physical parameter needed. The AAA calculation model consists of two components, the configuration and the actual dose calculation algorithm.

The configuration module is used to characterize the phase space of clinical beam. The phase space is done by a multiple source model consisting of a primary photon beam, extra focal photon source and electron contamination source.

The dose calculation module is divided into two parts. The first part is made as if the patient were a water equivalent medium. Firstly, the monoenergetic kernels in every beamlet are superpositioned to form polyenergetic pencil beam kernels for every voxel along the fanline. Then, the calculation model is separated the energy deposition along the fanline and perpendicular to the fanline. To account for the heterogeneous medium a correction is made scaled locally with the inverse relative electron density. The second part, electron contamination is modeled with a depth-dependence curve that describes the total amount of electron contamination dose at a certain depth. Electron contamination is used to model the photon contamination.

3.1.5 Collapse Cone Convolution (CCC)

The CCC method uses an analytical kernel represented by a set of cones, the energy deposited in which is collapse into a line. The CCC algorithm determines the total energy released per unit mass (TERMA) in a 3D matrix of the irradiated volume, based on the ray-tracing technique. The TERMA contained two parts namely, the primary and scatter part. The dose in a voxel of irradiated volume is determined by

convolving the point kernel with the TERMA distribution. Contaminated electron entering to phantom in the build-up region that modeled by using an exponential function. This contaminated electron dose is added to the photon dose.

3.2 AAA and CCC calculations in treatment planning

Chow et al [1] studied the evaluation of dose calculation in tangential photon beam by AAA and CCC algorithms compared with Monte Carlo in a solid water phantom. The photon beams of 6 and 15 MV with field sizes 4×4, 10×10 and 20×20 cm^2 with gantry rotated in 5° and 45° anti-clockwise were used in this study and vertical dose profiles at a distance of 2 mm from the phantom lateral skin (skin slab) was calculated. The results in the gantry 0° were found that both AAA and CCC overestimated doses in the phantom skin profile compared to Mante Carlo. For oblique photon beam at 5°, the mean doses in skin slab were underestimated in both AAA and CCC when compared with Monte Carlo. However, the mean doses in skin slab were overestimated in both AAA and CCC in oblique photon beam at 45°. This study was found that both AAA and CCC cannot predict doses reliably at depth shallower than 2 mm which is related to surface doses.

Hasenbalg et al [2] studied the difference doses of AAA and CCC calculations in clinical cases when compared with Monte Carlo. Five clinical cases were studied: three lung and two breast cases. Each clinical case was calculated in AAA, CCC and Monte Carlo. The planning target volume (PTV) coverage in each clinical case was found and compared. The results showed that CCC algorithm performed overall better than AAA compared to Monte Carlo, but AAA remains an attractive option for routine use in the clinic due to its short computation times. Dose difference between the difference algorithms for the median value of the PTV were typically 0.4% in the lung and -1.3% in the breast.

3.3 Surface dosimetry

Chow and Grigorov [3] studied the effect of beam obliquity on the surface dose profiles for tangential photon beams. The 6 and 15 MV photon beams with

10×10 cm^2 field sizes produced by a Varian 21 EX linear accelerator were used. Monte Carlo simulations were created base on the EGSnrc code and verified with film measurement. Firstly, the relative dose profiles in the phantom skin (2 mm depth from the surface) of the half phantom geometry (HPG) were calculated for increasing gantry angles from 270° to 280° clockwise. The results showed that when the beam angle starting from 270° to 273°, was increased from 1° to 3°, the relative depth doses in phantom skin were increased from 68% to 79% and 81% to 87% at 10 cm depth with 6 and 15 MV photon beams, respectively. After that, the relative dose profile of full phantom enclosing the whole tangential beam (full phantom geometry, or FPG) were also calculated with Monte Carlo for increasing gantry angles from 270° to 280° clockwise. The results showed that the relative dose profiles in the phantom skin did not change significantly with an oblique tangential beam. In this study shown the relative depth doses were sensitive increased to the beam obliquity for the HPG or phantom-air interface medium. The prediction of surface relative dose variation for tangential beam should be cautions in radiation therapy.

The study of Alashrah et al [4] was to investigate the dose at the surface of a water phantom at depth of 0.007 cm as a recommended by the International Commission on Radiological Protection and International Commission on Radiation Units and Measurement by using radiochromic films (Gafchromic MD-55 film), thermoluminescent dosimeters (TLD-100 chip) and ionization chamber (PTW 0.6-cm^3 Farmer chamber) in a 6-MV photon beam. The results were compared with the calculation using the Monte Carlo simulation software (MCNP5, BEAMnrc and DOSXYZnrc). The percent surface dose (PSD) was 15.0 ± 3.6%, 16.0 ± 5.0% and 50.0 ± 3.0% for radiochromic films, TLDs and ionisation chamber, respectively. The calculation using MCNP5 and DOSXYZnrc yielded a percent surface dose of 15.0 ± 2.0% and 15.7 ± 2.2%. The results showed good agreement between using radiochromic film and TLDs with the Monte Carlo simulation. However, the cylindrical ionisation was overestimated of the percent surface dose when compared with both Monte Carlo simulations.

Wong et al [5] studied the accuracy of surface dose calculation by a clinically using treatment planning system and measurement by thermoluminescent dosimeters in a customized chest wall phantom. A CMS Xio 3D treatment planning

system (Elekta CMS Software, Stockholm, Sweden) was used to calculation the seven points doses that were placed throughout each right chest wall phantom and were measured by thermoluminescent dosimeters (LiF chips). The results showed that there was no significant difference between measured doses (TLDs) and calculated doses (TPS). Dose accuracy of up to 2.21% was obtained.

CHAPTER IV
MATERIALS AND METHODS

4.1 Materials

4.1.1 Linear accelerator

ClinaciX linear accelerator which manufactured by Varian Oncology Systems, Palo Alto, California, USA was used in this study as shown in Figure 4.1. This machine is dual photon beam energies as 6 and 10 MV, the field size can be changed from 0.3 x 0.3 cm^2 to 40 x 40 cm^2 at 100 cm source to surface distance. The machine can also generate five electron beam energies as 6 MeV, 9 MeV, 12MeV, 16 MeV and 20 MeV. The dose rate ranges from 100 - 600 monitor units per minute. The MLCs are 120 leafs Millenium with of tungsten-alloy composition.

Figure 4.1 The Varian ClinaciX linear accelerator.

4.1.2 Treatment planning system

The analytical anisotropic algorithm (AAA) version 8.9 available in Eclipse treatment planning system (Varian, Palo Alto, California, USA) and the

collapsed cone convolution algorithm (CCC) version 9.2 available in Pinnacle treatment planning system (Philips, Fitchburg, Wisconsin, USA) were used for planning and calculation in this study.

4.1.3 CT simulator

The GE Optima CT580 Healthcare CT 16 slices (General Electric Healthcare, Milwaukee, Wisconsin, USA) with spiral computed tomography system was used to scan the slice images of the phantom as shown in Figure 4.2. The gantry aperture diameter is 80 cm but the true size scan field is 60 cm.

Figure 4.2 The GE Optima CT580 Healthcare in Ramathibodi Hospital.

4.1.4 Rando phantom

The Alderson Rando phantom (RSD, Long beach, California, USA) is an invaluable aid in radiotherapy treatment planning. The soft tissue material is manufactured with a proprietary urethane formulation and has an elective atomic number and mass density which simulates muscle tissue which randomly distributed fat. The lung material has the same elective atomic number and mass density which simulates lungs in a median respiratory state. The Rando phantom is sliced at 2.5 cm thicknesses and 3 cm thick sections for only breast part. Each phantom section is hole grid pattern and can be inserted the TLD into its. The Alderson Rando phantom with right breast is shown in Figure 4.3.

Figure 4.3 The Alderson Rando phantom.

4.1.5 Thermoluminescent dosimeter

4.1.5.1 Thermoluminescent dosimeter type 100 rods

TLD-100 rods is made from Lithium Fluoride (Li natural) doped with magnesium and titanium (LiF:Mg.Ti) that manufactured by Harshaw Chemical Company, Cleveland, Ohio, USA. The measurement ranges are 10 pGy to 10 Gy. The diameter is 1 mm and 5 mm length.

4.1.5.2 Thermoluminescent reader

The TLD annealing oven (PTW-TLDO) was used to heat the TLDs before and after reading. HARSHAW TLD Model 5500 Automatic Reader was used by inserted the planchet that consists 50 rods maximum and controlled by WinREMS program. The TLD annealing oven and TLD Reader is shown in Figure 4.4.

Figure 4.4 The TLD annealing oven (left) and TLD Reader (right).

4.1.6 Superflab bolus material

Superflab bolus is made from synthetic oil gel that has a specific gravity of 1.02. It is a tissue equivalent sheet that uses to place on the patient surface to avoid the skin sparing effect or to compensate the irregular shape in hot spot area. There are various thicknesses of bolus but in this study, the 5mm and 10 mm thicknesses of bolus were used as shown in Figure 4.5.

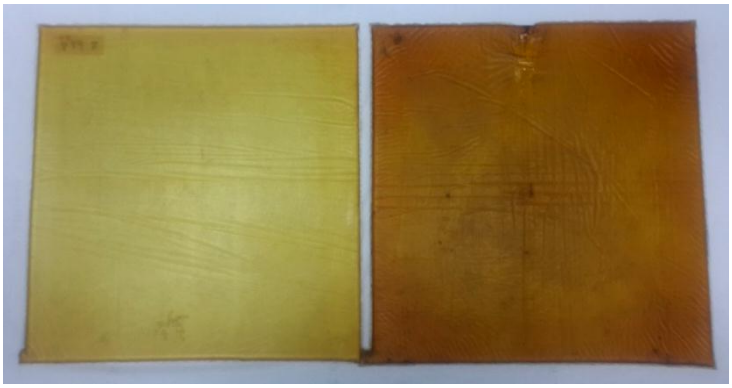

Figure 4.5 The 5 mm (left) and 10 mm (right) thicknesses of bolus.

4.2 Methods

There are 3 main procedures of this study.

4.2.1 TLD preparation and calibration

4.2.1.1 TLD preparation

Cobalt-60 teletherapeutic machine (Theratron Elite 80 unit) was used to irradiate radiation dose for TLDs. Firstly, all of 200 rods TLD were irradiated and annealed 4 times for responsibility. The annealing was done by TLD heating with 400 °C for 1 hour and 100 °C for 2 hours in TLD annealing oven (PTW-TLDO). TLDs were calibrated at dose 200 cGy at the depth of maximum dose 0.5 cm (D_{max} = 0.5 cm), field size 15x15 cm^2 and SAD technique 80 cm with bolus 0.5 cm covered.

4.2.1.2 TLD calibration

After annealing all of 200 TLDs for nullifying the residual background, 200 cGy of radiation dose was irradiated by Cobalt-60 machine. Then,

Irradiated TLDs were heated at 100 °C for 10 minutes to eliminate off-peak noise in TLD annealing oven (PTW-TLDO). After that, TLDs were read out by the TLD reader (HARSHAW TLD Model 5500 Automatic Reader) with heated at 260 °C in reading process and the charge of TLDs were showed in nanocoulomb (nC). The irradiation was done 2 times and the average of charge reading in each TLD was found. Then, TLDs were selected and divided into each group follow their uniformity (±10%) to giving dose of 200 cGy.

4.2.1.3 Linearity test of TLD

TLDs were irradiated with the dose 50, 100 and 300 cGy. The reading of charge was averaged and converted to absolute dose and plotted on a linear scale as a function of irradiated dose.

4.2.2 Treatment Planning

Firstly, TLDs were put in rod holders and put into totally 13 holds in breast Rando phantom follow these points

- Four points in the right upper breast Rando phantom slab. There was a superior point (B1), a medial point (B2), an inferior point (B3) and a lateral point (B4).
- Four points in the right lower breast Rando phantom slab. There was a superior point (B5), a medial point (B6), an inferior point (B7) and a lateral point (B8).
- Two points in Lung Rando phantom slab that close to the breast phantom. There was a lateral point (L1) and a medial point (L2).

And the other three points of TLDs with holder free were placed on breast Rando phantom surface under bolus covered (5 and 10 mm). There was a lateral point (S1), a center point (S2) and a medial point (S3). The TLDs' points are shown in Figure 4.6.

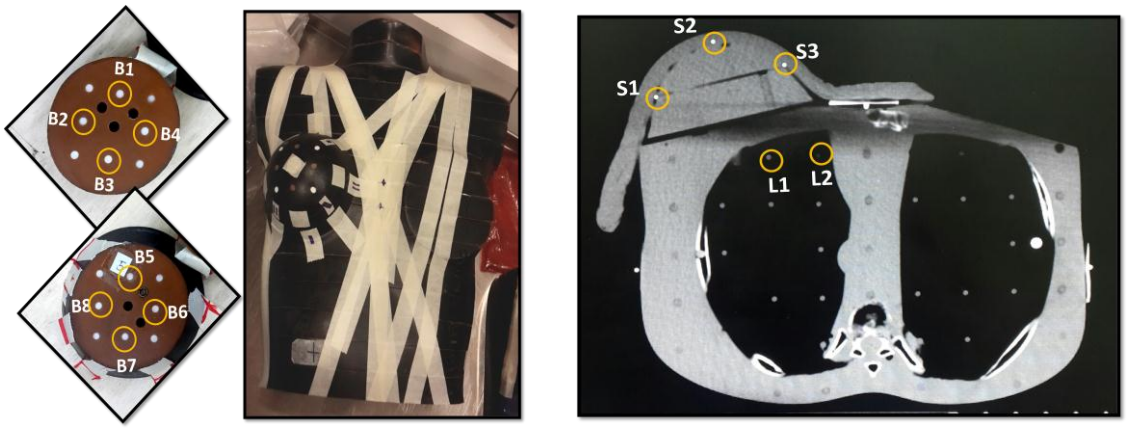

Figure 4.6 The points of TLD in breast Rando phantom slab (left) and the points of TLD in lung and on the surface with bolus covered (right).

After that, CT scan was used to scan the breast Rando phantom with 5 and 10 mm thicknesses bolus covered and obtained the slice images of the breast Rando phantom. Images were sent to treatment planning system both Eclipse and Pinnacle. The planning was done by SAD technique with Varian ClinaciX 6 MV photon beams and prescribed 200 cGy per fraction to 100% of point dose at point B6. Opposing tangential field technique with no wedge was planned with 69° in medial gantry angle and 240° in lateral gantry angle. Field sizes were 5 and 7.9 cm for X1 and X2 asymmetric jaw respectively and 16 cm symmetric Y in a medial field and 7.9 and 5 cm for X1 and X2 asymmetric jaw respectively and 16 cm symmetric Y jaw in a lateral field shown in Table 4.1. Both Eclipse and Pinnacle were planned by the same technique and calculated with dose contribution method at a prescription point. The doses in planning were calculated by the tool in the treatment planning system 3 times per each point and the comparisons of average dose in 13 points between Eclipse (AAA) and Pinnacles (CCC) were analyzed.

Table 4.1 A parameter of technique planning in both thicknesses of bolus and both algorithms.

Beam set up									
Beam	Collimators (cm)				Gantry (°)	MU per fraction			
						Bolus 5 mm		Bolus 10 mm	
	X1	X2	Y1	Y2		Pinnacle	Eclipse	Pinnacle	Eclipse
Med	5.0	7.9	8.0	8.0	69	114	111	117	113
Lat	7.9	5.0	8.0	8.0	240	107	105	106	106

4.2.3 Irradiation and measurement

TLDs were put into the points and placed on the surface points followed the figure 4.6. Varian ClinaciX was used to irradiate the breast Rando phantom that put TLDs inside as shown in Figure 4.7. The irradiation was done by opposing tangential fields technique followed the beam set up planning in both AAA and CCC algorithms seen in table 4.1. The irradiation was done 3 times for each algorithm. Finally, TLDs were read by Harshaw TLD reader and converted to average doses for each point. The comparisons of all 13 points between both algorithms planning and TLD measurements were found.

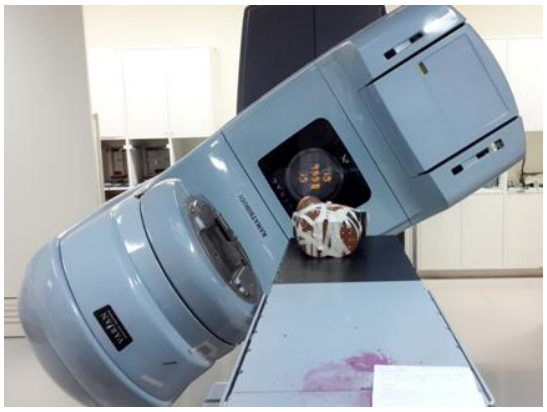

Figure 4.7 The Varian ClinaciX in irradiation process.

CHAPTER V
RESULTS AND DISCUSSION

5.1 TLD preparation and calibration

TLDs were selected (170 out of 200 rods) and separated into 3 groups followed their uniformity (±10%) to give the dose of 200 cGy. The linearity test was found by a linear relation of R^2 in all groups which shows in figure 5.1, 5.2 and 5.3.

Table 5.1 Irradiated doses and the average of absolute doses from TLD group 1 reading.

Irradiated Doses (cGy)	Average Doses ± SD (cGy)	%Diff
50	46.20 ± 1.16	-7.6 %
100	90.28 ± 2.60	-9.72 %
200	200	0 %
300	281.25 ± 8.35	-6.25 %

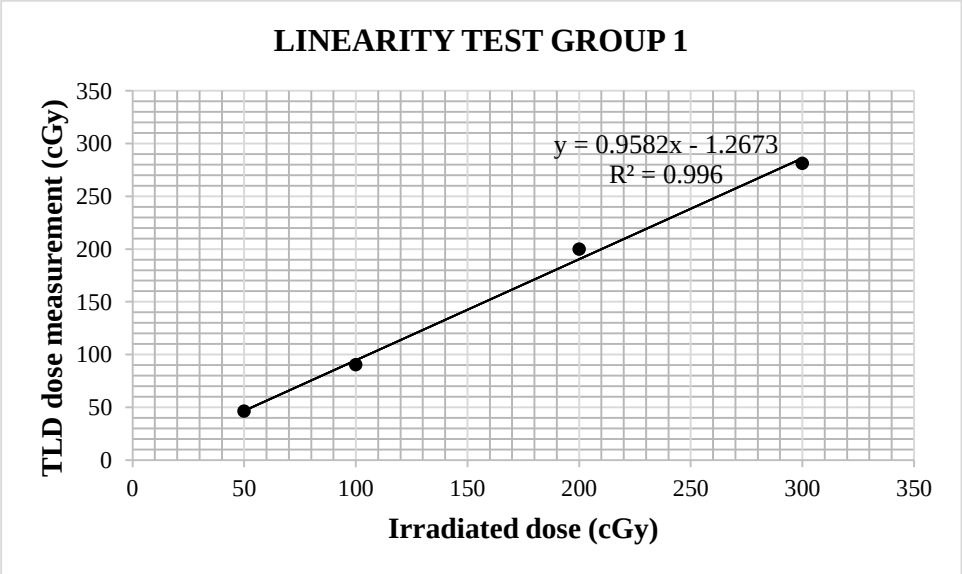

Figure 5.1 The linearity test for TLD group 1.

Table 5.2 Irradiated doses and the average of absolute doses from TLD group 2 reading.

Irradiated Doses (cGy)	Average Doses ± SD (cGy)	% Diff
50	47.41 ± 1.11	-5.18 %
100	92.10 ± 2.86	-7.9 %
200	200	0 %
300	285.55 ± 9.88	-4.82 %

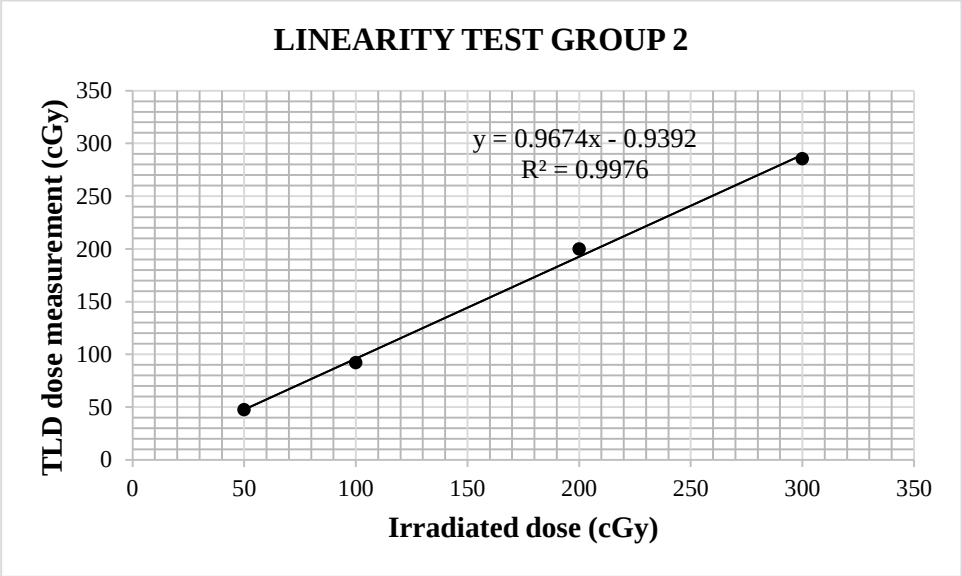

Figure 5.2 The linearity test for TLD group 2.

Table 5.3 Irradiated doses and the average of absolute doses from TLD group 3 reading.

Irradiated Doses (cGy)	Average Doses ± SD (cGy)	% Diff
50	47.61 ± 0.72	-4.78 %
100	93.44 ± 1.92	-6.56 %
200	200	0 %
300	293.88 ± 8.15	-2.04 %

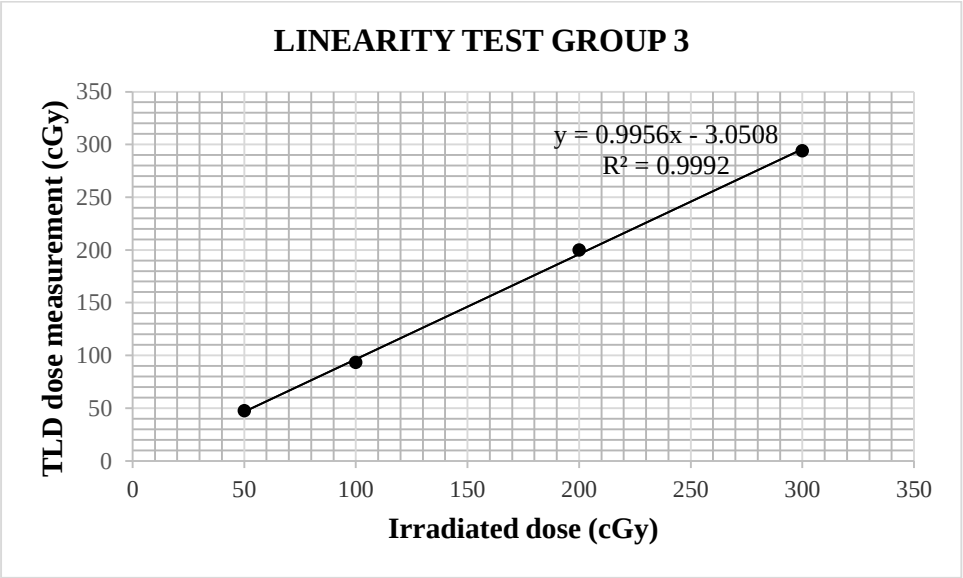

Figure 5.3 The linearity test for TLD group 3.

5.2 Radiation doses in treatment planning

The results in Table 5.4 show the doses on breast Rando phantom surface with bolus covered (point S1, S2, and S3) that were closely matched in both algorithms and both thicknesses of the bolus. The differences were between -0.21 to 1.33% in 5 mm thicknesses of bolus and 0 to 0.10% in 10 mm thicknesses of bolus. The doses in breast Rando phantom (Point B1 to B8) were also well matched in both algorithms and both thicknesses of the bolus in which the differences were -0.2 to 1.16% in 5 mm thicknesses of bolus and -0.15 to 0.90% in 10 mm thicknesses of bolus. The lung does in point L1 were somewhat similar with 0.95% and 0.42% differences at 5mm and 10 mm bolus thicknesses. Nevertheless, overestimate doses in a lung (point L2) were found in AAA with 2.42% and 6.06% differences at 5 mm and 10 mm bolus thicknesses, respectively when compared with CCC algorithm. The graphs in Figure 5.4 shown that the percentage difference at L2 in 10 mm bolus thicknesses was clearly higher than 5 mm bolus thicknesses. In the prescription point (B6) of 200 cGy has shown the difference in 5 mm thicknesses of bolus was -0.20% and -0.01% in 10 mm thicknesses of bolus.

The planning doses in both algorithms and both bolus thicknesses were not difference at point S1 to L1, however point L2 was not. The planning dose by CCC algorithm was less at both thicknesses of bolus when compared with AAA algorithm

at point L2 which is heterogeneous lung region. As a result of high percentage differences at point L2 may cause from the point of low doses.

Table 5.4 A comparison of point doses in treatment planning by AAA algorithm (Eclipse) versus CCC algorithm (Pinnacle) in breast Rando phantom with 5 and 10 mm bolus covered.

POINTS	Bolus 5 mm			Bolus 10 mm		
	AAA (cGy) ± SD	CCC (cGy) ± SD	% Diff	AAA (cGy) ± SD	CCC (cGy) ± SD	% Diff
S1	189.9 ± 0.4	187.4 ± 0.5	1.33	199.2 ± 0.5	199.0 ± 1.0	0.10
S2	202.5 ± 0.6	202.1 ± 0.9	0.20	208.6 ± 0.4	208.5 ± 0.5	0.05
S3	186.2 ± 0.3	186.6 ± 0.4	-0.21	195.3 ± 0.5	195.3 ± 0.7	0
B1	209.3 ± 0.2	206.9 ± 0.4	1.16	207.9 ± 0.4	207.1 ± 0.8	0.39
B2	203.2 ± 0.7	203.5 ± 0.5	-0.15	204.2 ± 0.5	203.2 ± 0.6	0.49
B3	209.4 ± 0.6	207.6 ± 0.6	0.87	209.9 ± 0.7	207.9 ± 0.9	0.96
B4	206.0 ± 0.3	204.9 ± 0.5	0.54	206.1 ± 0.6	204.8 ± 0.8	0.63
B5	201.8 ± 0.5	202.1 ± 0.2	-0.15	200.8 ± 0.4	200.4 ± 0.4	0.20
B6	200.1 ± 0.3	200.5 ± 0.3	-0.20	200.0 ± 0.3	200.2 ± 0.6	-0.01
B7	203.6 ± 0.6	203.5 ± 0.6	0.05	202.2 ± 0.4	202.1 ± 0.8	0.05
B8	200.9 ± 0.2	201.2 ± 0.5	-0.15	200.0 ± 0.3	200.3 ± 0.8	-0.15
L1	191.9 ± 0.5	190.1 ± 0.5	0.95	188.8 ± 0.5	188.0 ± 0.9	0.42
L2	80.3 ± 0.5	78.4 ± 0.5	2.42	89.2 ± 0.8	84.1 ± 0.8	6.06

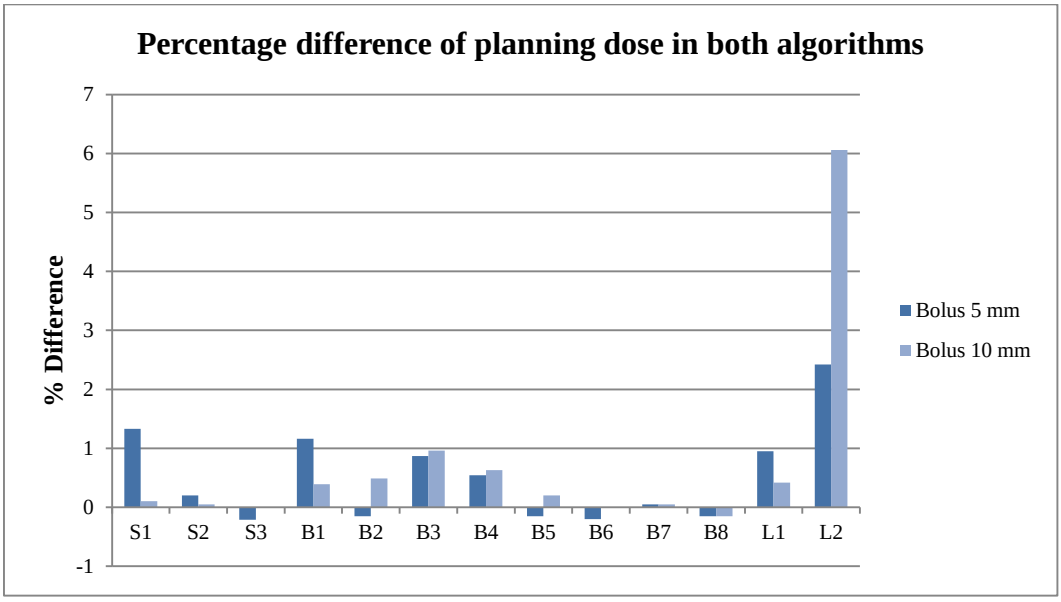

Figure 5.4 The percentage difference of point doses in treatment planning between AAA and CCC at both bolus thicknesses.

5.3 Irradiated doses measurement

The irradiated TLDs were read in charge particle and converted to average doses shown in Table 5.5 and 5.6. The planning doses on breast Rando phantom surface with bolus covered (point S1, S2 and S3) were overestimated in both algorithms when compared with irradiated doses in which the differences were ranged between 6.1% to 12.3% and 3.1% to 8.3% at 5 and 10 mm bolus thicknesses, respectively. Same as the results of Chung et al [6] that showed the overestimated in surface and build-up doses in both treatment planning systems. The percentage differences in build-up region (point S1 to S3) were less than 15% that showed the good agreement with the study of Fraass et al [7] which recommended that the commissioning tolerance dose must not over 15% in complexity heterogeneous media in build-up region.

The planning doses in breast Rando phantom (Point B1 to B8) were overestimated in both algorithms when compared with irradiated doses which the differences were ranged between 10.3% to 18.1% and 4.4% to 12.9% at 5 and 10 mm bolus thicknesses, respectively.

The planning doses in lung (Point L1) were also overestimated in both algorithms when compared with irradiated dose which the differences were 14.1% and 15.3% at 5 mm bolus thicknesses, the differences were 8.3% and 6.6% at 10 mm bolus thicknesses. However, the planning doses in lung (point L2) were underestimated in both algorithms at 10 mm bolus thicknesses when compared with irradiated dose seen in Figure 5.6. Although the planning doses in lung (point L2) in CCC algorithm were underestimated at 5 mm bolus thicknesses, they were overestimated in AAA algorithm shown in Figure 5.5.

The percentage differences in breast Rando phantom and lung (point L1) were up to 18.1%. The high differences between planning doses and irradiated doses cause from the TLD calibration errors that large up to 9.72% differences as shown in Table 5.2. The other reasons cause from the irradiation process that different TLDs were used at the same point in irradiation repetition and also from the air gap between bolus and breast Rando phantom.

Table 5.5 A comparison of point doses from treatment planning doses versus TLD measurements in breast Rando phantom with 5 mm bolus thicknesses covered in both algorithms.

POINTS	AAA			CCC		
	Irradiated dose (cGy) ± SD	Planning dose (cGy) ± SD	% Diff	Irradiated dose (cGy) ± SD	Planning dose (cGy) ± SD	% Diff
S1	178.9 ± 3.9	189.9 ± 0.4	6.1	176.5 ± 10.3	187.4 ± 0.5	6.2
S2	185.4 ± 1.1	202.5 ± 0.6	9.2	192.3 ± 7.8	202.1 ± 0.9	5.1
S3	165.8 ± 3.6	186.2 ± 0.3	12.3	169.3 ± 5.7	186.6 ± 0.4	10.2
B1	177.2 ± 6.3	209.3 ± 0.2	18.1	185.0 ± 3.5	206.9 ± 0.4	11.8
B2	179.2 ± 7.7	203.2 ± 0.7	13.4	176.1 ± 3.8	203.5 ± 0.5	15.6
B3	186.9 ± 13.5	209.4 ± 0.6	12.0	183.8 ± 9.0	207.6 ± 0.6	12.9
B4	178.1 ± 3.7	206.0 ± 0.3	15.7	185.6 ± 9.0	204.9 ± 0.5	10.4
B5	176.6 ± 5.5	201.8 ± 0.5	14.3	176.1 ± 5.4	202.1 ± 0.2	14.8
B6	181.4 ± 7.9	200.1 ± 0.3	10.3	180.8 ± 6.3	200.5 ± 0.3	10.9
B7	182.9 ±3.3	203.6 ± 0.6	11.3	183.0 ± 5.6	203.5 ± 0.6	11.2
B8	180.2 ± 5.3	200.9 ± 0.2	11.5	174.6 ± 5.3	201.2 ± 0.5	15.2
L1	168.1 ± 8.2	191.9 ± 0.5	14.1	164.9 ± 4.3	190.1 ± 0.5	15.3
L2	77.0 ± 11.8	80.3 ± 0.3	4.3	94.8 ± 17.4	78.4 ± 0.5	-17.3

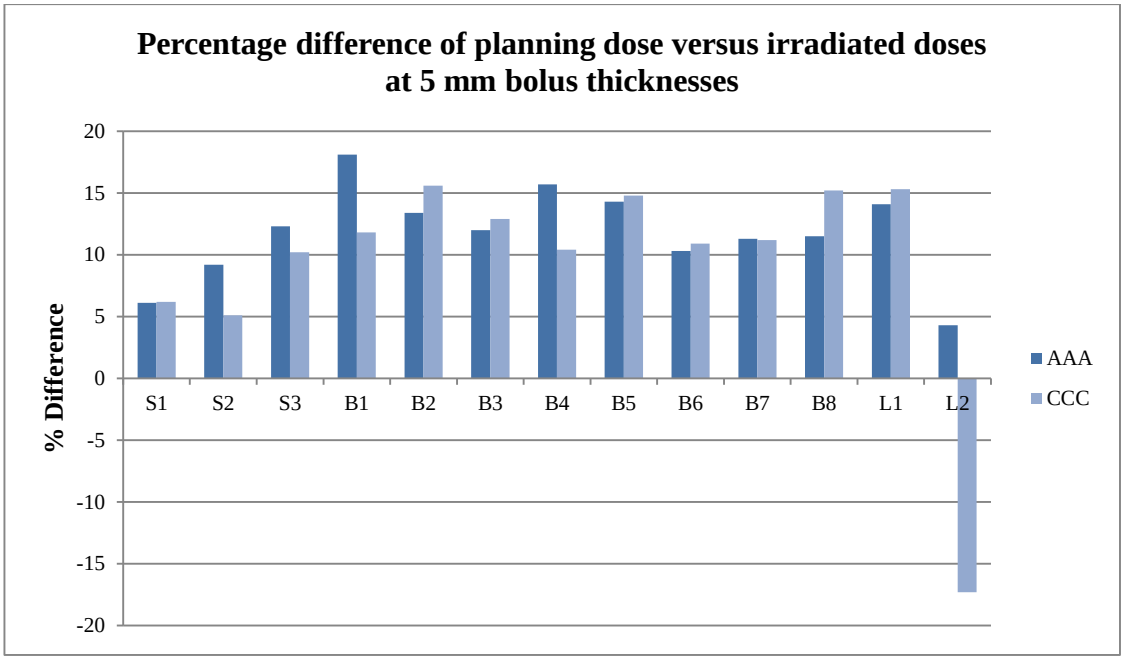

Figure 5.5 The graph of percentage difference between planning doses versus irradiated doses in both algorithms at 5 mm bolus thicknesses.

Table 5.6 A comparison of point doses from treatment planning doses versus TLD measurements in breast Rando phantom with 10 mm bolus thicknesses covered in both algorithms.

POINTS	AAA			CCC		
	Irradiated dose (cGy) ± SD	Planning dose (cGy) ± SD	% Diff	Irradiated dose (cGy) ± SD	Planning dose (cGy) ± SD	% Diff
S1	186.1 ± 10.3	199.2 ± 0.5	7.0	191.2 ± 8.1	199.0 ± 1.0	4.1
S2	194.1 ± 2.2	208.6 ± 0.4	7.5	194.4 ± 2.8	208.5 ± 0.5	7.3
S3	180.4 ± 5.3	195.3 ± 0.5	8.3	189.4 ± 5.8	195.3 ± 0.7	3.1
B1	194.4 ± 8.9	207.9 ± 0.4	6.9	192.9 ± 4.3	207.1 ± 0.8	7.4
B2	189.6 ± 8.1	204.2 ± 0.5	7.7	189.8 ± 7.8	203.2 ± 0.6	7.1
B3	195.7 ± 11.1	209.9 ± 0.7	7.3	197.6 ± 6.1	207.9 ± 0.9	5.2
B4	186.9 ± 4.9	206.1 ± 0.6	10.3	187.8 ± 6.3	204.8 ± 0.8	9.1
B5	186.2 ± 6.8	200.8 ± 0.4	7.8	190.7 ± 6.2	200.4 ± 0.4	5.1
B6	185.0 ± 5.1	200.0 ± 0.3	8.1	189.7 ± 6.1	200.2 ± 0.6	5.5
B7	187.2 ± 8.9	202.2 ± 0.4	8.0	190.0 ± 7.6	202.1 ± 0.8	6.4
B8	177.1 ± 1.1	200.0 ± 0.3	12.9	191.8 ± 6.6	200.3 ± 0.8	4.4
L1	174.3 ± 5.7	188.8 ± 0.5	8.3	176.3 ± 9.9	188.0 ± 0.9	6.6
L2	105.7 ± 19.8	89.2 ± 0.8	-15.6	105.6 ± 15.3	84.1 ± 0.8	-20.4

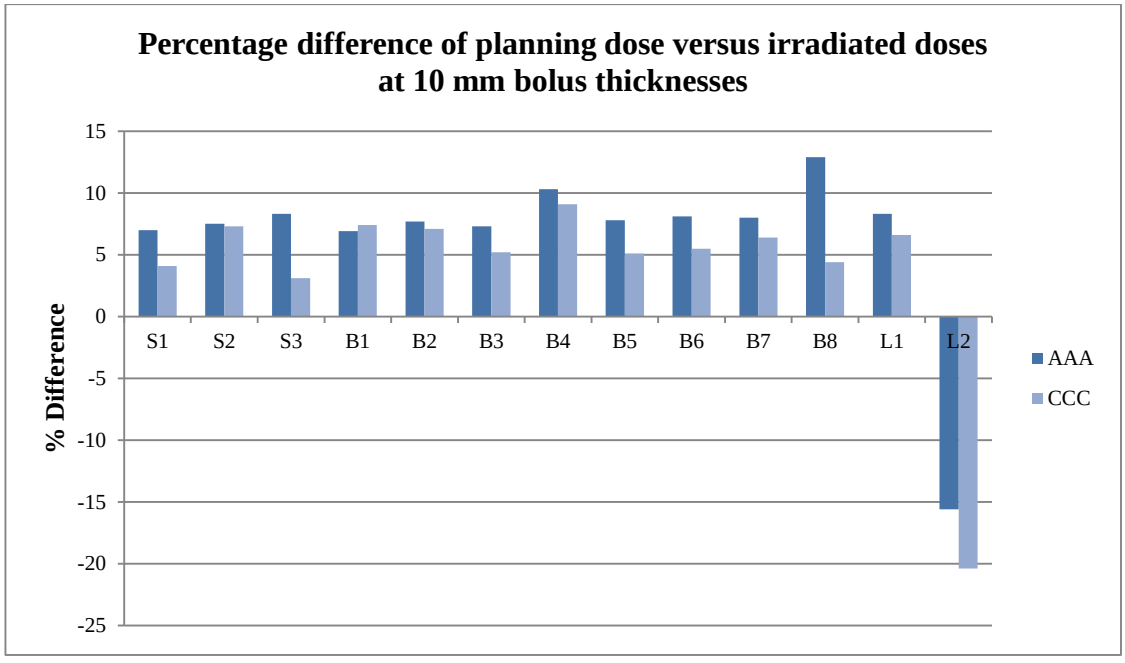

Figure 5.6 The graph of percentage difference between planning doses versus irradiated doses in both algorithms at 10 mm bolus thicknesses.

It seems that the percentage differences of planning doses versus irradiated doses at lung (point L2) were different compared with the other points. It might due to point L2 was located at the point of beam edges region (seen in Figure 5.7) which leads to large uncertainty as fully illustrated with large standard deviation at both bolus thicknesses shown in Table 5.2 and 5.3.

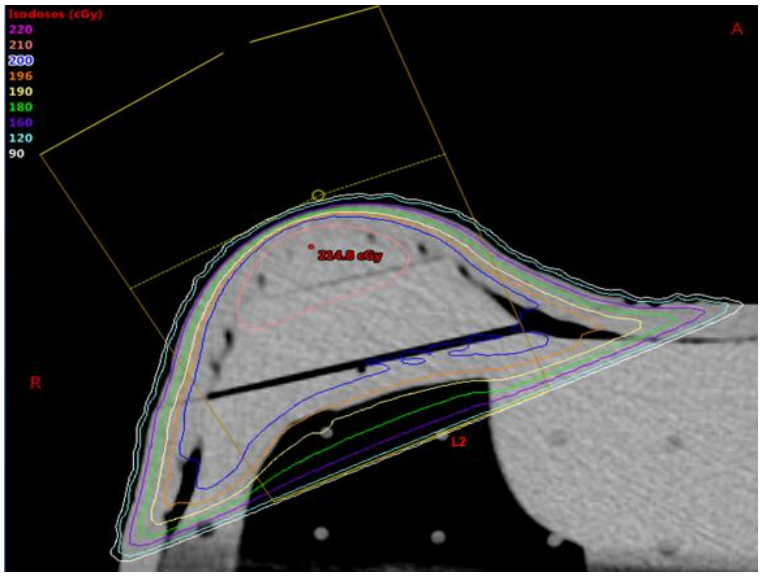

Figure 5.7 The lung point L2 which located through the beam edges.

Above all, the CCC algorithm performed better in TLD measurements as shown in Table 5.2 and 5.3 which the average percentage differences between planning doses and irradiation doses were less than the AAA algorithm.

CHAPTER VI
CONCLUSIONS

In this study, both algorithms were not difference in treatment planning calculation of build-up region, breast Rando phantom and lung (point L1) in which the differences doses were less than 2%. The planning doses in build-up region, breast Rando phantom and lung (point L1) were overestimated in both thicknesses of the bolus and both algorithm when compared with irradiated dose except in lung (point L2) that was a point of beam edges region. However, the TLD measurements show that CCC algorithm performed overall better when compared with AAA algorithm at both thicknesses of the bolus.

The limitation of this study might cause the uncertainties in measurement. The process of placing bolus over the curve of breast Rando phantom might be the main cause of dose measurement errors from the air gap between bolus and surface of the phantom. In this study, 3 times repetition for measurements were done and TLDs were changed with bolus covered every time. This process might be the main limitation of this study and made the measurement errors. Another limitation is the grid hold pattern and small hold size in Rando phantom. The small size and many holds using in this study were difficult to find the fitted detector to put into all of the holds rather than TLD.

Further study might be required in other detectors or other techniques to have more evidence to illustrate the accuracy of dose calculation in build-up region and in lung tissue from the algorithms. The radiochromic film can be used by placing between the slabs of breast Rando phantom to measure the doses in any depths of breast phantom due to its small size and high resolution. The study of Alashrah et al [4] shown that radiochromic film (Gafchromic MD-55 film) and TLD-100 have a good agreement in surface dose and dose in the region after d_{max} measurement when compared with Monte Carlo results.

REFERENCES

1. Chow JCL, Jiang R, Leung MKK. Dosimetry of oblique tangential photon beams calculation by superposition/convolution algorithms: A Monte Carlo evaluation. J Appl Clin Med Phys 2011;12:108-21.
2. Hasenbalg F, Neuenschwander H, Mini R, Born EJ. Collapsed cone and analytical anisotropic algorithm dose calculation compared to VMC++ Monte Carlo simulations in clinical cases. J Phys Conf Ser 2007;74:1-1.
3. Chow JCL, Grigorov GN. Surface dosimetry for oblique tangential photon beams: A Monte carlo simulation study. Med Phys 2008;35:70-6.
4. Alashrah S, Kandaiya S, Maalej N, Taher AE. Skin dose measurements using radiochromic films, tlds and ionisation chamber and comparison with Monte Carlo simulation. Radiat Prot Dosimetry 2013:1-7.
5. Wong S, Back M, Tan PW, Lee KM, Baggarley S, Lu JJ. Can radiation therapy treatment planning system accurately predict surface doses in postmastectomy radiation therapy patients?. Med Dosim 2012;37:163-9.
6. Chung H, Jin H, Dempsey JF, Liu C, Palta J,Suh TS, et al. Evaluation of surface and build-up region dose for intensity-modulated radiation therapy in head and neck cancer. Med Phys 2005;32:2682-9.
7. Fraass B, Doppke K, Hunt M, Kutcher G, Starkschall G, Stern R, et al. American association of physicists in medicine radiation therapy committee task group 53: quality assurance for clinical radiotherapy treatment planning. Med Phys 1998;25:1773-828.
8. Esch AV, Tillikainen L, Pyykkonen J, Tenhunen M, Helminen H, Siljamaki S, et al. Testing of the analytical anisotropic algorithm for photon dose calculation. Med Phys 2006;33:4130-48.
9. Ahnesjo A. Collapsed cone convolution of radiant energy for photon dose calculation in heterogeneous media. Med Phys 1989;16:577-92.

10. Nakano M, Hill RF, Whitaker M, Kim JH, Kuncic Z. A study of surface dosimetry for breast cancer radiotherapy treatments using gafchromic EBT2 film. J Appl Clin Med Phys 2012;13:83-97.
11. Kry SF, Price M, Followill D, Mourtada F, Salehpour M. The use of LiF (TLD-100) as an out-of-field dosimeter. J Appl Clin Med Phys 2007;8:169-75.
12. Gagne IM, Zavgorodni S. Evaluation of the analytical anisotropic algorithm in an extreme water-lung interface phantom using Monte carlo dose calculations. J Appl Clin Med Phys 2006;8:33-46.
13. Jaffray DA, editor. Comparison of AAA and CCC algorithms for H&N RapidArc pre-treatment QA. World Congress on Medical Physics and Biomedical Engineering; 2015 June 7-12; Toronto, Canada. Switzerland: Springer International;2015.
14. Attix FH. Introduction to radiological physics and radiation dosimetry. Wisconsin: John Wiley & Sons; 1986.
15. Mayles P, Nahum A, Rosenwald JC. Handbook of raiotherapy physics. Vol.1. New York: Taylor & Francis; 2007.
16. Apipanyasopon L. Fundamental to advanced radiotherapy treatment techniques. 10th SEACOMP and 12th AOCMPl; 2012 Dec 11-14; Chiang Mai, Thailand.
17. Sakulsingharoj S. Risk estimation of radiation induced second cancers for three dimensional conformal radiotherapy (3D-CRT) and intensity modulated radiotherapy (IMRT) [dissertation]. Bangkok: Mahidol University; 2009.
18. Rukthung K. Assessing the accuracy of surface and build-up doses calculated from beam comissioning of breast technique using EDGE™ detector [dissertation]. Bangkok: Mahidol University; 2015.
19. Josefsson A. Evaluation of the anisotropic amalytic algoritm (AAA) for 6 MV photon energy [dissertation]. Gothenburg: Gothenburg University; 2008.
20. Nilsson E. Evaluation of the anisotropic amalytic algoritm (AAA) in lung tumours for 6 MV photon energy [dissertation]. Gothenburg: Gothenburg University; 2009.

APPENDIX

1. TLD Calibration

After annealing all of 200 TLDs with 400 °C for 1 hour and 100 °C for 2 hours, 200 cGy of radiation dose was irradiated by Cobalt-60 machine. Irradiated TLDs were heated at 100 °C for 10 minutes to eliminate off-peak noise. Then, TLDs were heated at 260 °C in reading process and the charge of TLDs reading was showed in nanocoulomb (nC). The Element Correction Coefficient (ECC_i) of individual TLD (seen in table 1.1, 1.2 and 1.3) was calculated by this equation below (where $\bar{Q}$ is the average charge of all TLD and Q_i is the individual charge).

$$ECC_i = \frac{\bar{Q}}{Qi}$$

After that, the TLDs that showed uniformity (±10%) to giving dose of 200 cGy were selected and separated into 3 groups. Each group was selected the standard TLDs that ECC_i value close to 1 (1% of all TLDs in each group). (* seen in the table means the standard TLD selected.)

Table A.1 The ECC_i value of each TLD in group 1.

No.	TLD no.	Charge reading (nC)			ECC_i	%Diff
		1st	2nd	Q_i		
1	154	5390.442	5141.189	5265.8155	0.912274	-9.6161846
2	190	5123.094	5389.916	5256.505	0.9138899	-9.422372
3	124	5282.293	5220.155	5251.224	0.914809	-9.3124397
4	17	5189.129	5303.338	5246.2335	0.9156792	-9.2085547
5	19	5241.13	5237.17	5239.15	0.9169172	-9.0611005
6	83	5251.57	5186.139	5218.8545	0.920483	-8.638618
7	183	5207.466	5208.065	5207.7655	0.922443	-8.4077831
8	148	5294.951	5104.729	5199.84	0.923849	-8.2428014
9	70	5262.178	5115.641	5188.9095	0.9257951	-8.015266
10	177	5223.022	5149.844	5186.433	0.9262371	-7.9637137
11	138	5259.48	5089.409	5174.4445	0.9283831	-7.7141544
12	120	5195.803	5112.015	5153.909	0.9320822	-7.2866758

Table A.1 The ECC_i value of each TLD in group 1. (cont.)

No.	TLD no.	Charge reading (nC)			ECC_i	%Diff
		1st	2nd	Q_i		
13	170	5238.239	4964.903	5101.571	0.9416446	-6.1971785
14	77	5107.415	5040.113	5073.764	0.9468053	-5.6183323
15	29	5084.64	4854.261	4969.4505	0.9666797	-3.4468837
16	168	5049.803	4851.091	4950.447	0.9703905	-3.0512961
17	18	4924.147	4970.286	4947.2165	0.9710242	-2.9840482
18	68	4965.262	4921.334	4943.298	0.9717939	-2.9024785
19	54	4984.725	4887.805	4936.265	0.9731785	-2.7560756
20	35	5010.051	4849.27	4929.6605	0.9744823	-2.6185926
21	30	5009.937	4840.985	4925.461	0.9753131	-2.5311734
22	110	4916.843	4927.912	4922.3775	0.9759241	-2.4669856
23	96	4948.486	4831.568	4890.027	0.9823804	-1.7935593
24	22	4956.05	4810.849	4883.4495	0.9837036	-1.6566384
25	23	4951.615	4764.008	4857.8115	0.9888953	-1.1229433
26*	93	4894.398	4803.809	4849.1035	0.9906711	-0.9416727
27*	78	4855.098	4761.822	4808.46	0.9990448	-0.0956146
28*	21	4883.407	4729.939	4806.673	0.9994162	-0.0584154
29*	42	4861.29	4741.714	4801.502	1.0004925	0.049227
30*	88	4767.691	4809.352	4788.5215	1.0032046	0.3194364
31	100	4731.927	4738.395	4735.161	1.0145097	1.4302187
32	65	4760.257	4676.104	4718.1805	1.0181609	1.7836943
33	131	4775.177	4597.324	4686.2505	1.0250982	2.4483672
34	62	4731.412	4627.601	4679.5065	1.0265755	2.5887541
35	140	4765.064	4568.19	4666.627	1.0294088	2.8568611
36	159	4777.058	4523.244	4650.151	1.0330561	3.1998348
37	43	4671.896	4622.322	4647.109	1.0337323	3.2631588
38	149	4702.228	4526.524	4614.376	1.0410653	3.9445473
39	169	4709.184	4511.023	4610.1035	1.0420301	4.0334861

Table A.1 The ECC_i value of each TLD in group 1. (cont.)

No.	TLD no.	Charge reading (nC)			ECC_i	%Diff
		1st	2nd	Q_i		
40	115	4718.166	4482.801	4600.4835	1.0442091	4.2337415
41	171	4688.495	4506.393	4597.444	1.0448995	4.2970134
42	37	4600.27	4579.443	4589.8565	1.0466268	4.4549591
43	66	4615.953	4543.623	4579.788	1.0489278	4.6645506
44	151	4717.843	4439.544	4578.6935	1.0491785	4.6873344
45	153	4617.757	4385.353	4501.555	1.0671572	6.2930929
46	145	4577.209	4416.438	4496.8235	1.06828	6.3915865
47	157	4580.188	4342.889	4461.5385	1.0767288	7.1260989
48	125	4461.998	4444.398	4453.198	1.0787454	7.2997195
49	174	4515.076	4383.177	4449.1265	1.0797326	7.3844741
50	119	4411.621	4447.435	4429.528	1.0845099	7.7924475
51	166	4521.911	4322.571	4422.241	1.0862969	7.9441378
52	139	4465.941	4357.024	4411.4825	1.0889461	8.1680928
53	116	4470.39	4330.939	4400.6645	1.091623	8.3932864
54	80	4456.334	4321.503	4388.9185	1.0945445	8.6377978
55	182	4397.654	4281.747	4339.7005	1.1069581	9.6623474
56	193	4421.07	4246.711	4333.8905	1.1084421	9.7832917

Table A.2 The ECC_i value of each TLD in group 2.

No.	TLD no.	Charge reading (nC)			ECC_i	%Diff
		1st	2nd	Q_i		
1	60	6556.403	6434.607	6495.505	0.9088497	-10.029192
2	123	6475.943	6459.149	6467.546	0.9127786	-9.5555862
3	20	6493.421	6298.887	6396.154	0.9229668	-8.346257
4	188	6462.355	6287.501	6374.928	0.9260399	-7.9867038
5	127	6408.589	6336.71	6372.6495	0.926371	-7.9481077
6	136	6420.207	6286.79	6353.4985	0.9291633	-7.6237035

Table A.2 The ECC_i value of each TLD in group 2. (cont.)

No.	TLD no.	Charge reading (nC)			ECC_i	%Diff
		1st	2nd	Q_i		
6	136	6420.207	6286.79	6353.4985	0.9291633	-7.6237035
7	185	6342.299	6252.846	6297.5725	0.9374148	-6.6763572
8	162	6364.898	6174.352	6269.625	0.9415935	-6.2029466
9	163	6326.9	6158.074	6242.487	0.9456869	-5.7432484
10	117	6223.588	6238.181	6230.8845	0.9474478	-5.5467103
11	103	6225.132	6148.867	6186.9995	0.9541682	-4.8033299
12	38	6137.009	6091.587	6114.298	0.9655136	-3.5718187
13	192	6175.224	5957.742	6066.483	0.9731236	-2.7618669
14	15	6025.957	6104.211	6065.084	0.9733481	-2.7381689
15	47	6083.716	5999.832	6041.774	0.9771034	-2.3433142
16	107	6080.363	5937.619	6008.991	0.9824341	-1.7879937
17	133	6055.792	5947.201	6001.4965	0.983661	-1.6610423
18	181	5991.931	5931.289	5961.61	0.9902422	-0.9853936
19*	31	5909.413	5934.519	5921.966	0.9968713	-0.3138527
20*	46	5913.861	5918.089	5915.975	0.9978808	-0.2123695
21*	16	5828.452	5993.968	5911.21	0.9986852	-0.1316538
22*	113	5952.273	5827.082	5889.6775	1.0023364	0.2330913
23*	135	5924.779	5797.48	5861.1295	1.0072185	0.7166739
24	172	5951.878	5690.708	5821.293	1.0141111	1.3914756
25	128	5866.488	5775.411	5820.9495	1.014171	1.3972943
26	82	5864.702	5761.372	5813.037	1.0155514	1.5313263
27	89	5831.373	5791.659	5811.516	1.0158172	1.557091
28	160	5851.57	5685.488	5768.529	1.0233871	2.2852599
29	27	5833.581	5645.314	5739.4475	1.0285725	2.7778796
30	164	5808.296	5581.084	5694.69	1.0366566	3.5360396
31	141	5737.769	5630.076	5683.9225	1.0386204	3.7184333
32	51	5710.401	5637.386	5673.8935	1.0404562	3.8883173

Table A.2 The ECC_i value of each TLD in group 2. (cont.)

No.	TLD no.	Charge reading (nC)			ECC_i	%Diff
		1st	2nd	Q_i		
33	50	5657.221	5641.444	5649.3325	1.0449797	4.3043631
34	1	5712.634	5549.243	5630.9385	1.0483932	4.6159442
35	150	5709.161	5529.702	5619.4315	1.0505401	4.8108645
36	155	5703.283	5460.229	5581.756	1.0576309	5.4490605
37	152	5734.833	5427.947	5581.39	1.0577003	5.4552602
38	180	5609.186	5530.196	5569.691	1.059922	5.6534329
39	112	5599.308	5504.422	5551.865	1.0633252	5.9553925
40	86	5540.083	5552.964	5546.5235	1.0643492	6.0458737
41	158	5582.694	5412.462	5497.578	1.0738252	6.8749753
42	189	5549.836	5314.078	5431.957	1.0867976	7.986548
43	137	5455.125	5397.442	5426.2835	1.0879339	8.082653
44	134	5437.89	5341.506	5389.698	1.0953189	8.7023851

Table A.3 The ECC_i value of each TLD in group 3.

No.	TLD no.	Charge reading (nC)			ECC_i	%Diff
		1st	2nd	Q_i		
1	39	4219.784	4186.253	4203.0185	0.925007	-8.1072854
2	156	4324.378	4071.32	4197.849	0.9261462	-7.9743189
3	191	4300.146	4079.434	4189.79	0.9279276	-7.7670306
4	106	4245.064	4129.036	4187.05	0.9285348	-7.6965541
5	142	4245.627	4112.875	4179.251	0.9302676	-7.4959533
6	57	4208.242	4116.437	4162.3395	0.9340472	-7.0609668
7	130	4206.684	4103.944	4155.314	0.9356265	-6.8802615
8	114	4179.58	4124.416	4151.998	0.9363737	-6.7949695
9	87	4151.917	4136.854	4144.3855	0.9380936	-6.5991658
10	14	4128.302	4146.735	4137.5185	0.9396506	-6.4225373
11	44	4127.828	4106.562	4117.195	0.9442889	-5.8997896

Table A.3 The ECC_i value of each TLD in group 3. (cont.)

No.	TLD no.	Charge reading (nC)			ECC_i	%Diff
		1st	2nd	Q_i		
11	44	4127.828	4106.562	4117.195	0.9442889	-5.8997896
12	59	4160.523	4071.832	4116.1775	0.9445224	-5.8736181
13	176	4162.506	4051.716	4107.111	0.9466074	-5.6404156
14	109	4087.891	4124.951	4106.421	0.9467665	-5.6226678
15	45	4104.703	4069.911	4087.307	0.951194	-5.1310301
16	49	4085.387	4080.234	4082.8105	0.9522415	-5.015374
17	178	4171.873	3989.864	4080.8685	0.9526947	-4.9654232
18	73	4106.324	4034.709	4070.5165	0.9551175	-4.6991558
19	3	4036.924	4042.278	4039.601	0.9624272	-3.9039676
20	28	4085.991	3986.53	4036.2605	0.9632237	-3.8180455
21	67	4035.636	4034.178	4034.907	0.9635468	-3.7832316
22	146	4096.652	3963.198	4029.925	0.964738	-3.6550879
23	76	4045.973	4007.552	4026.7625	0.9654957	-3.5737441
24	105	4049.823	3983.539	4016.681	0.967919	-3.3144344
25	56	4050.389	3944.41	3997.3995	0.9725877	-2.8184883
26	10	4006.287	3977.105	3991.696	0.9739774	-2.6717866
27	194	4032.733	3915.714	3974.2235	0.9782595	-2.2223704
28	84	4002.111	3940.24	3971.1755	0.9790103	-2.1439718
29	90	3986.052	3927.657	3956.8545	0.9825536	-1.7756164
30	75	3970.297	3940.522	3955.4095	0.9829126	-1.7384491
31	111	3966.053	3922.319	3944.186	0.9857095	-1.4497656
32	72	3948.625	3937.731	3943.178	0.9859615	-1.4238384
33	121	3978.978	3895.323	3937.1505	0.9874709	-1.268803
34	91	3949.558	3889.754	3919.656	0.9918783	-0.818821
35*	40	3958.366	3851.121	3904.7435	0.9956663	-0.4352514
36*	165	3956.715	3828.356	3892.5355	0.998789	-0.1212453
37*	81	3928.479	3847.26	3887.8695	0.9999877	-0.0012295

Table A.3 The ECC_i value of each TLD in group 3. (cont.)

No.	TLD no.	Charge reading (nC)			ECC_i	%Diff
		1st	2nd	Q_i		
38*	144	3973.401	3748.941	3861.171	1.0069022	0.6854918
39*	41	3922.396	3794.829	3858.6125	1.0075699	0.7512999
40	173	3906.819	3792.563	3849.691	1.0099049	0.9807729
41	104	3885.366	3806.493	3845.9295	1.0108926	1.0775237
42	102	3877.706	3746.982	3812.344	1.0197982	1.9413879
43	161	3871.659	3747.169	3809.414	1.0205826	2.0167514
44	132	3872.817	3721.451	3797.134	1.0238832	2.3326095
45	25	3802.956	3733.22	3768.088	1.0317757	3.0797117
46	8	3781.277	3712.993	3747.135	1.0375451	3.618651
47	5	3727.301	3761.689	3744.495	1.0382766	3.6865554
48	108	3747.649	3684.46	3716.0545	1.046223	4.4180833
49	184	3770.447	3626.386	3698.4165	1.0512125	4.8717563
50	36	3744.456	3637.615	3691.0355	1.0533146	5.0616056
51	11	3689.284	3668.274	3678.779	1.0568239	5.3768592
52	9	3667.289	3591.352	3629.3205	1.0712258	6.6489983
53	64	3613.847	3644.01	3628.9285	1.0713415	6.6590811
54	34	3637.512	3614.108	3625.81	1.0722629	6.7392931
55	52	3678.953	3572.428	3625.6905	1.0722983	6.7423668
56	71	3638.704	3602.63	3620.667	1.073786	6.871578
57	7	3645.855	3570.42	3608.1375	1.0775148	7.1938536
58	74	3594.66	3522.072	3558.366	1.0925862	8.4740434
59	4	3553.226	3546.555	3549.8905	1.0951948	8.6920447
60	92	3543.678	3536.706	3540.192	1.0981952	8.9415032
61	53	3587.048	3486.059	3536.5535	1.099325	9.0350903
62	24	3578.23	3457.931	3518.0805	1.1050974	9.5102407
63	94	3536.837	3444.774	3490.8055	1.113732	10.21179
64	79	3552.479	3425.652	3489.0655	1.1142874	10.256545

Table A.3 The ECC_i value of each TLD in group 3. (cont.)

No.	TLD no.	Charge reading (nC)			ECC_i	%Diff
		1st	2nd	Q_i		
65	6	3510.041	3432.9	3471.4705	1.1199351	10.709113

The standard TLDs were annealed and irradiated with 200 cGy (repeated the upper step) and the individual reading was calculated as Q_{ci} (the correct charge integral) according to the equation below

$$Q_{ci} = Q_i \times ECC_i$$

The average of Q_{ci} ($\overline{Q}_c$) for standard TLDs was used for determination of the reader calibration factor (RCF) by the equation below, where D is the giving dose of 200 cGy.

$$RCF = \frac{\overline{Q}c}{D}$$

The rest of TLDs except standard TLDs were annealed and irradiated with 200 cGy radiation dose to determine the individual element correction coefficient (ECC_{ci}) seen in table 1.4, 1.5 and 1.6 (where Q_i is the charge of individual TLD and D is the dose of 200 cGy).

$$ECC_{ci} = \frac{RCF \times D}{Qi}$$

ECC_{ci} for each TLD, RCF for standard TLDs and the charge of individual TLD (Q_i) used for calculation the unknown dose (D_u) according to the equation below

$$D_u = \frac{Qi \times ECCci}{RCF}$$

Table A.4 The ECC_{ci} value of each TLD in group 1.

TLD	Charge reading (nC)			ECC_i	Q_{ci}	ECC_{ci}
	1st	2nd	Q_i			
1	4954.053	4643.436	4798.745	0.912274		0.957814
2	5248.407	5064.593	5156.5	0.91389		0.891361
3	5026.659	4654.782	4840.721	0.914809		0.949508

Table A.4 The ECC_{ci} value of each TLD in group 1. (cont.)

TLD	Charge reading (nC)			ECC_i	Q_{ci}	ECC_{ci}
	1st	2nd	Q_i			
4	5028.391	4936.542	4982.467	0.915679		0.922496
5	5054.65	4998.899	5026.775	0.916917		0.914364
6	5164.974	4986.318	5075.646	0.920483		0.90556
7	5119.15	4963.479	5041.315	0.922443		0.911727
8	4994.032	4914.737	4954.385	0.923849		0.927725
9	4986.153	5029.146	5007.65	0.925795		0.917857
10	5025.014	4914.043	4969.529	0.926237		0.924897
11	4971.597	4905.835	4938.716	0.928383		0.930668
12	5004.328	4909.813	4957.071	0.932082		0.927222
13	4686.604	4373.455	4530.03	0.941645		1.01463
14	4881.292	4732.612	4806.952	0.946805		0.956178
15	4722.354	4620.908	4671.631	0.96668		0.983876
16	4556.13	4247.809	4401.97	0.970391		1.044147
17	4697.436	4586.037	4641.737	0.971024		0.990212
18	4761.19	4586.28	4673.735	0.971794		0.983433
19	4747.019	4618.189	4682.604	0.973179		0.98157
20	4739.414	4660.933	4700.174	0.974482		0.977901
21	4872.244	4792.727	4832.486	0.975313		0.951126
22	4816.395	4899.644	4858.02	0.975924		0.946127
23	4796.026	4817.899	4806.963	0.98238		0.956176
24	4633.908	4621.735	4627.822	0.983704		0.99319
25	4602.092	4460.573	4531.333	0.988895		1.014338
26*	4688.442	4548.573	4618.508	0.990671	4575.422	0.995192
27*	4600.52	4513.509	4557.015	0.999045	4552.662	1.008622
28*	4511.25	4496.34	4503.795	0.999416	4501.166	1.02054
29*	4652.522	4562.407	4607.465	1.000493	4609.734	0.997578
30*	4726.845	4727.929	4727.387	1.003205	4742.536	0.972272

Table A.4 The ECC_{ci} value of each TLD in group 1. (cont.)

TLD	Charge reading (nC)			ECC_i	Q_{ci}	ECC_{ci}
	1st	2nd	Q_i			
31	4619.795	4655.604	4637.7	1.01451		0.991074
32	4538.891	4580.752	4559.822	1.018161		1.008001
33	4438.032	4333.212	4385.622	1.025098		1.048039
34	4439.733	4543.377	4491.555	1.026576		1.023321
35	4347.342	4157.171	4252.257	1.029409		1.080909
36	4253.935	4026.33	4140.133	1.033056		1.110183
37	4453.862	4168.065	4310.964	1.033732		1.066189
38	4581.067	4144.313	4362.69	1.041065		1.053548
39	4376.629	4017.419	4197.024	1.04203		1.095134
40	4368.196	4108.246	4238.221	1.044209		1.084489
41	4412.648	4125.216	4268.932	1.0449		1.076687
42	4579.896	4613.729	4596.813	1.046627		0.999889
43	4421.792	4370.649	4396.221	1.048928		1.045513
44	4348.149	4187.948	4268.049	1.049179		1.07691
45	4077.469	4024.712	4051.091	1.067157		1.134584
46	4237.88	4171.058	4204.469	1.06828		1.093195
47	4165.729	4086.987	4126.358	1.076729		1.113889
48	4226.485	4112.688	4169.587	1.078745		1.10234
49	4188.023	3870.424	4029.224	1.079733		1.140742
50	4192.958	3952.171	4072.565	1.08451		1.128602
51	4224.363	4026.108	4125.236	1.086297		1.114192
52	4180.272	3989.133	4084.703	1.088946		1.125248
53	4239.72	4046.374	4143.047	1.091623		1.109402
54	4262.323	4127.79	4195.057	1.094545		1.095648
55	4119.073	4017.694	4068.384	1.106958		1.129762
56	4130.103	4030.812	4080.458	1.108442		1.126419

Table A.5 The ECC_{ci} value of each TLD in group 2.

TLD	Charge reading (nC)			ECC_i	Q_{ci}	ECC_{ci}
	1st	2nd	Q_i			
1	6194.053	6003.019	6098.536	0.90885		0.913296
2	6283.481	6026.262	6154.872	0.912779		0.904936
3	6016.488	5834.627	5925.558	0.922967		0.939956
4	6104.206	5935.282	6019.744	0.92604		0.92525
5	6241.892	5973.756	6107.824	0.926371		0.911907
6	6133.178	6025.833	6079.506	0.929163		0.916154
7	6127.067	6154.534	6140.801	0.937415		0.90701
8	6063.613	6044.421	6054.017	0.941594		0.920012
9	5951.139	5922.877	5937.008	0.945687		0.938144
10	6010.475	6161.599	6086.037	0.947448		0.915171
11	5908.148	6040.155	5974.152	0.954168		0.932311
12	5901.355	5990.774	5946.065	0.965514		0.936715
13	5704.908	5372.783	5538.846	0.973124		1.005582
14	5791.059	5665.788	5728.424	0.973348		0.972303
15	5759.913	5478.657	5619.285	0.977103		0.991188
16	5682.837	5501.939	5592.388	0.982434		0.995955
17	5818.852	5575.796	5697.324	0.983661		0.977611
18	5736.948	5543.964	5640.456	0.990242		0.987467
19*	5491.277	5628.096	5559.687	0.996871	5542.292	1.001813
20*	5356.17	5641.316	5498.743	0.997881	5487.09	1.012916
21*	5474.558	5780.536	5627.547	0.998685	5620.148	0.989732
22*	5461.593	5678.056	5569.825	1.002336	5582.838	0.999989
23*	5660.023	5492.39	5576.207	1.007219	5616.458	0.998845
24	5552.615	5490.931	5521.773	1.014111		1.008692
25	5506.852	5186.893	5346.873	1.014171		1.041687
26	5502.282	5204.877	5353.58	1.015551		1.040382
27	5593.449	5372.594	5483.022	1.015817		1.015821

Table A.5 The ECC_{ci} value of each TLD in group 2. (cont.)

TLD	Charge reading (nC)			ECC_i	Q_{ci}	ECC_{ci}
	1st	2nd	Q_i			
28	5498.064	5145.828	5321.946	1.023387		1.046566
29	5583.161	5357.394	5470.278	1.028573		1.018187
30	5420.699	5071.703	5246.201	1.036657		1.061676
31	5526.126	5240.562	5383.344	1.03862		1.034629
32	5407.24	5433.355	5420.298	1.040456		1.027576
33	5490.963	5517.833	5504.398	1.04498		1.011876
34	5414.385	5303.55	5358.968	1.048393		1.039336
35	5310.416	5238.496	5274.456	1.05054		1.055989
36	5075.459	4671.546	4873.503	1.057631		1.142867
37	5051.696	4669.397	4860.547	1.0577		1.145914
38	5124.001	4906.114	5015.058	1.059922		1.110609
39	5110.388	5125.691	5118.04	1.063325		1.088262
40	5346.036	5382.028	5364.032	1.064349		1.038354
41	5100.018	4971.226	5035.622	1.073825		1.106073
42	5105.301	4959.073	5032.187	1.086798		1.106828
43	5163.892	4978.588	5071.24	1.087934		1.098305
44	5157.861	5026.293	5092.077	1.095319		1.09381

Table A.6 The ECC_{ci} value of each TLD in group 3.

TLD	Charge reading (nC)			ECC_i	Q_{ci}	ECC_{ci}
	1st	2nd	Q_i			
1	3975.482	4018.091	3996.787	0.925007		0.909046
2	3874.669	3761.069	3817.869	0.926146		0.951647
3	3920.891	3810.954	3865.923	0.927928		0.939818
4	3953.186	3929.772	3941.479	0.928535		0.921802
5	4015.308	3971.901	3993.605	0.930268		0.90977
6	3893.636	3926.348	3909.992	0.934047		0.929225

Table A.6 The ECC_{ci} value of each TLD in group 3. (cont.)

TLD	Charge reading (nC)			ECC_i	Q_{ci}	ECC_{ci}
	1st	2nd	Q_i			
7	4053.253	3939.511	3996.382	0.935627		0.909138
8	3965.382	4045.244	4005.313	0.936374		0.907111
9	4152.895	4248.95	4200.923	0.938094		0.864872
10	3984.595	4102.892	4043.744	0.939651		0.89849
11	3841.265	3921.574	3881.42	0.944289		0.936065
12	3766.798	3853.181	3809.99	0.944522		0.953615
13	3799.275	3721.691	3760.483	0.946607		0.966169
14	3961.684	4145.204	4053.444	0.946767		0.89634
15	3854.799	3885.934	3870.367	0.951194		0.938738
16	3976.157	4111.39	4043.774	0.952242		0.898483
17	3916.045	3890.799	3903.422	0.952695		0.930789
18	4025.28	4117.075	4071.178	0.955118		0.892435
19	3814.629	3927.06	3870.845	0.962427		0.938623
20	3831.174	3973.184	3902.179	0.963224		0.931085
21	3791.766	3846.587	3819.177	0.963547		0.951321
22	3758.688	3748.353	3753.521	0.964738		0.967961
23	3814.366	3956.112	3885.239	0.965496		0.935145
24	3770.831	3837.375	3804.103	0.967919		0.95509
25	3670.369	3720.344	3695.357	0.972588		0.983197
26	3748.908	3773.561	3761.235	0.973977		0.965976
27	3816.98	3827.161	3822.071	0.97826		0.9506
28	3786.035	3855.622	3820.829	0.97901		0.950909
29	3809.448	3892.44	3850.944	0.982554		0.943473
30	3791.454	3899.99	3845.722	0.982913		0.944754
31	3778.916	3916.716	3847.816	0.98571		0.94424
32	3817.92	3778.323	3798.122	0.985962		0.956594
33	3732.432	3694.302	3713.367	0.987471		0.978428

Table A.6 The ECC_{ci} value of each TLD in group 3. (cont.)

TLD	Charge reading (nC)			ECC_i	Q_{ci}	ECC_{ci}
	1st	2nd	Q_i			
34	3826.612	3879.83	3853.221	0.991878		0.942916
35*	3700.412	3770.938	3735.675	0.995666	3719.486	0.972585
36*	3555.877	3488.412	3522.145	0.998789	3517.879	1.031548
37*	3668.467	3597.698	3633.083	0.999988	3633.038	1.000049
38*	3591.927	3508.248	3550.088	1.006902	3574.591	1.023429
39*	3724.583	3662.138	3693.361	1.00757	3721.319	0.983728
40	3644.144	3533.063	3588.604	1.009905		1.012445
41	3655.343	3576.549	3615.946	1.010893		1.004789
42	3669.511	3659.355	3664.433	1.019798		0.991494
43	3615.102	3506.757	3560.93	1.020583		1.020313
44	3636.5	3488.604	3562.552	1.023883		1.019848
45	3712.08	3721.19	3716.635	1.031776		0.977568
46	3528.825	3473.362	3501.094	1.037545		1.037751
47	3558.99	3493.591	3526.291	1.038277		1.030335
48	3541.576	3451.992	3496.784	1.046223		1.03903
49	3509.073	3379.441	3444.257	1.051213		1.054875
50	3530.882	3436.459	3483.671	1.053315		1.042941
51	3566.877	3487.831	3527.354	1.056824		1.030025
52	3465.911	3314.912	3390.412	1.071226		1.071629
53	3512.263	3542.552	3527.408	1.071342		1.030009
54	3473.069	3432.545	3452.807	1.072263		1.052263
55	3480.434	3494.992	3487.713	1.072298		1.041732
56	3426.831	3377.635	3402.233	1.073786		1.067905
57	3423.338	3382.497	3402.918	1.077515		1.06769
58	3488.792	3515.522	3502.157	1.092586		1.037436
59	3317.408	3326.156	3321.782	1.095195		1.093769
60	3369.948	3393.538	3381.743	1.098195		1.074376

Table A.6 The ECC_{ci} value of each TLD in group 3. (cont.)

TLD	Charge reading (nC)			ECC_i	Q_{ci}	ECC_{ci}
	1st	2nd	Q_i			
61	3324.063	3401.503	3362.783	1.099325		1.080433
62	3373.408	3420.059	3396.734	1.105097		1.069634
63	3422.418	3416.011	3419.215	1.113732		1.062601
64	3345.966	3402.199	3374.083	1.114287		1.076815
65	3210.949	3281.842	3246.396	1.119935		1.119168

2. Treatment planning

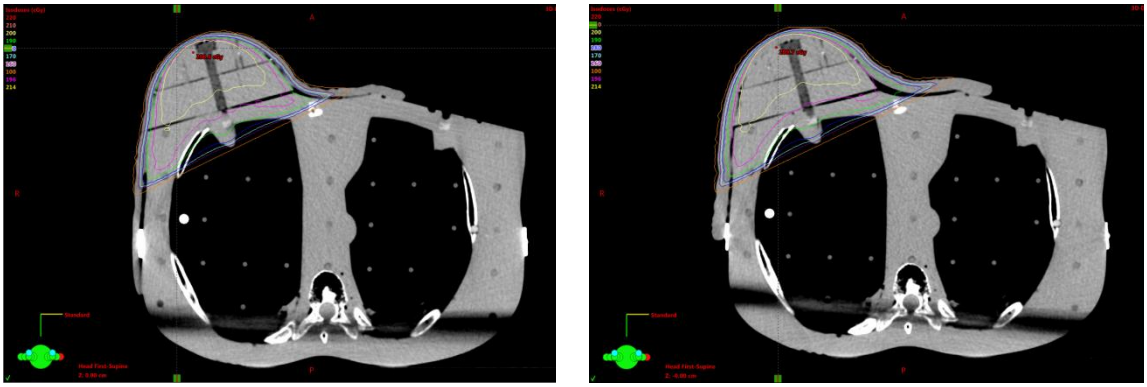

Figure A.1 The dose distribution in breast Rando phantom with 5 mm bolus covered (left) and 10 mm bolus covered (right) by AAA algorithm (Eclipse TPS).

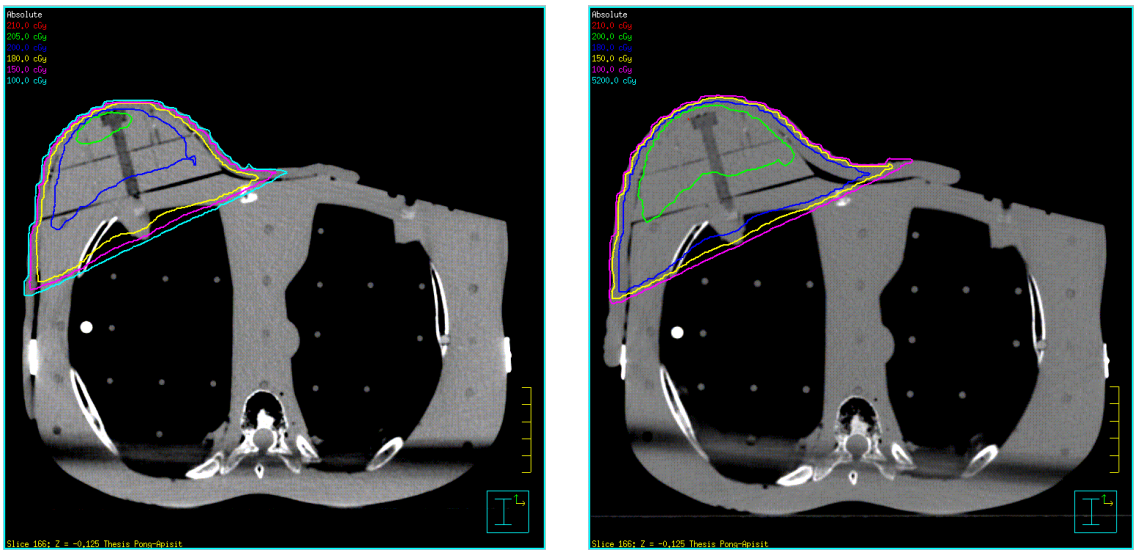

Figure A.2 The dose distribution in breast Rando phantom with 5 mm bolus covered (left) and 10 mm bolus covered (right) by CCC algorithm (Pinnacle TPS).

Table A.7 The point doses in treatment planning by both algorithms calculation with 5 mm bolus covered.

POINTS	AAA (cGy)				CCC (cGy)			
	1st	2nd	3rd	Average	1st	2nd	3rd	Average
S1	189.5	190	190.2	189.9 ± 0.4	187.1	188	187.2	187.4 ± 0.5
S2	202.6	201.9	203.1	202.5 ± 0.6	202.9	202.2	201.2	202.1 ± 0.9
S3	186.1	186.5	185.9	186.2 ± 0.3	187	186.7	186.2	186.6 ± 0.4
B1	209.4	209.5	209.1	209.3 ± 0.2	207.2	207.1	206.5	206.9 ± 0.4
B2	202.5	203.8	203.4	203.2 ± 0.7	203.6	203.9	202.9	203.5 ± 0.5
B3	209.2	210.1	209	209.4 ± 0.6	207.5	208.3	207.1	207.6 ± 0.6
B4	206.2	205.6	206.1	206.0 ± 0.3	205.4	204.8	204.4	204.9 ± 0.5
B5	202.2	201.9	201.2	201.8 ± 0.5	202.3	202.2	201.9	202.1 ± 0.2
B6	199.9	200.1	200.4	200.1 ± 0.3	200.9	200.4	200.3	200.5 ± 0.3
B7	203.9	202.9	203.9	203.6 ± 0.6	202.9	203.8	203.9	203.5 ± 0.6
B8	200.8	200.7	201.1	200.9 ± 0.2	200.8	201.7	201.2	201.2 ± 0.5
L1	192.3	191.4	192.1	191.9 ± 0.5	189.7	190.6	190.1	190.1 ± 0.5
L2	80.2	79.7	80.9	80.3 ± 0.5	78.3	78.9	78	78.4 ± 0.5

Table A.8 The point doses in treatment planning by both algorithms calculation with 10 mm bolus covered.

POINTS	AAA (cGy)				CCC (cGy)			
	1st	2nd	3rd	Average	1st	2nd	3rd	Average
S1	199.1	199.8	198.8	199.2 ± 0.5	198.4	198.5	200.1	199.0 ± 1.0
S2	208.9	208.7	208.1	208.6 ± 0.4	209.1	208.4	208.1	208.5 ± 0.5
S3	195.8	195.2	194.9	195.3 ± 0.5	195.1	194.8	196.1	195.3 ± 0.7
B1	208.3	207.9	207.6	207.9 ± 0.4	207.8	207.4	206.2	207.1 ± 0.8
B2	204.7	203.8	204.1	204.2 ± 0.5	203.6	202.5	203.4	203.2 ± 0.6
B3	210.5	209.2	209.8	209.9 ± 0.7	208.8	207.1	207.6	207.9 ± 0.9
B4	205.7	205.9	206.8	206.1 ± 0.6	204.9	203.9	205.5	204.8 ± 0.8
B5	200.3	201.1	200.9	200.8 ± 0.4	200.8	200.1	200.2	200.4 ± 0.4
B6	199.7	199.9	200.3	200.0 ± 0.3	199.5	200.5	200.6	200.2 ± 0.6
B7	202.5	201.8	202.3	202.2 ± 0.4	202.2	201.3	202.8	202.1 ± 0.8
B8	200.3	199.9	199.7	200.0 ± 0.3	199.4	200.6	200.9	200.3 ± 0.8
L1	189.2	188.2	188.9	188.8 ± 0.5	187.1	188.9	187.9	188.0 ± 0.9
L2	90.1	88.6	89	89.2 ± 0.8	85	83.8	83.6	84.1 ± 0.8

3. TLDs Measurement

Table A.9 The irradiated doses in breast Rando phantom with 5 mm bolus covered by both algorithms calculation.

POINTS	AAA (cGy)				CCC (cGy)			
	1st	2nd	3rd	Average	1st	2nd	3rd	Average
S1	174.9	182.6	179.2	178.9 ± 3.9	170.3	170.7782	188.3	176.5 ± 10.3
S2	186.5	185.3	184.2	185.4 ± 1.1	185.4	190.6576	200.8	192.3 ± 7.8
S3	164.4	169.8	162.9	165.8 ± 3.6	165.1	175.8265	166.9	169.3 ± 5.7
B1	171.1	183.6	176.6	177.2 ± 6.3	181.9	188.7961	183.9	185.0 ± 3.5
B2	170.3	183.4	183.9	179.2 ± 7.7	171.8	179.1703	177.2	176.1 ± 3.8
B3	189.1	199.1	172.3	186.9 ± 13.5	178.9	178.2922	194.1	183.8 ± 9.0
B4	179.0	181.2	174.0	178.1 ± 3.7	176.6	185.2024	194.7	185.6 ± 9.0
B5	175.1	172.0	182.7	176.6 ± 5.5	181.1	170.466	176.5	176.1 ± 5.4
B6	187.8	172.6	183.8	181.4 ± 7.9	180.4	174.6582	187.2	180.8 ± 6.3
B7	181.2	180.5	186.6	182.9 ±3.3	176.6	185.1983	187.0	183.0 ± 5.6

Table A.9 The irradiated doses in breast Rando phantom with 5 mm bolus covered by both algorithms calculation. (cont.)

POINTS	AAA (cGy)				CCC (cGy)			
	1st	2nd	3rd	Average	1st	2nd	3rd	Average
B8	174.1	183.4	183.0	180.2 ± 5.3	171.5	171.3879	180.7	174.6 ± 5.3
L1	158.6	173.5	172.0	168.1 ± 8.2	162.7	162.0311	169.8	164.9 ± 4.3
L2	77.0	65.1	88.7	77.0 ± 11.8	77.7	112.5481	94.0	94.8 ± 17.4

Table A.10 The irradiated doses in breast Rando phantom with 10 mm bolus covered by both algorithms calculation.

POINTS	AAA (cGy)				CCC (cGy)			
	1st	2nd	3rd	Average	1st	2nd	3rd	Average
S1	187.9	175.0	195.3	186.1 ± 10.3	200.6	186.4	186.5	191.2 ± 8.1
S2	196.3	193.8	191.8	194.1 ± 2.2	195.7	196.2	191.2	194.4 ± 2.8
S3	181.5	174.6	184.9	180.4 ± 5.3	196.1	186.9	185.2	189.4 ± 5.8
B1	184.2	201.0	197.8	194.4 ± 8.9	195.4	187.9	195.3	192.9 ± 4.3
B2	197.8	181.6	189.3	189.6 ± 8.1	195.6	192.7	180.9	189.8 ± 7.8
B3	204.4	183.2	199.4	195.7 ± 11.1	200.1	202.0	190.6	197.6 ± 6.1
B4	192.1	186.0	182.5	186.9 ± 4.9	195.0	185.1	183.2	187.8 ± 6.3
B5	189.5	178.4	190.7	186.2 ± 6.8	197.6	188.8	185.5	190.7 ± 6.2
B6	182.8	181.3	190.7	185.0 ± 5.1	196.0	189.2	183.9	189.7 ± 6.1
B7	193.0	176.9	191.6	187.2 ± 8.9	198.6	184.4	186.8	190.0 ± 7.6
B8	178.1	176.0	177.0	177.1 ± 1.1	192.6	197.8	184.7	191.8 ± 6.6
L1	169.0	180.3	173.4	174.3 ± 5.7	179.4	165.2	184.2	176.3 ± 9.9
L2	127.9	98.7	90.2	105.7 ± 19.8	90.5	121.1	104.9	105.6 ± 15.3

BIOGRAPHY

NAME	Mr. Pongapisit Masunun
DATH OF BIRTH	08 January 1989
PLACE OF BIRTH	Chiang Mai, Thailand
INSTITUTIONS ATTENDED	Chiang Mai University, 2007: Bachelor of Science (Radiologic Technology) Mahidol University, 2011: Master of Science (Medical Physics)
RESEARCH GRANTS	Graduate Studies of Mahidol University Alumni Association
HOME ADDRESS	998/248 B-Republic condo Sukhumvit 101/1, Bangjak, Prakanong, Bangkok, Thailand, 10260 Tel. 089-9518400 Email: newzoozwen@gmail.com
PUBLICATION / PRESENTATION	13th South-East Asian Congress of Medical Physics (SEACOMP 2015) Yogyakarta, Indonesia